UNIVERSITY OF GAZİANTEP

GRADUATE SCHOOL OF

NATURAL & APPLIED SCIENCES

INCREASING WIND TURBINE EFFICIENCY

M. Sc. THESIS

IN

AIRCARFT AND AEROSPACE ENGINEERING

BY

TUKA FATTAL

SEPTEMBER 2018

Increasing Wind Turbine Efficiency

M.Sc. Thesis

in

Aircraft and Aerospace Engineering

University of Gaziantep

Supervisor

Prof. Dr. İbrahim H. GÜZELBEY

by

TUKA FATTAL

September 2018

REPUBLIC OF TURKEY

UNIVERSITY OF GAZİANTEP

GRADUATE SCHOOL OF NATURAL & APPLIED SCIENCES

AIRCRAFT AND AEROSPACE ENGINEERING DEPARTMENT

Name of the thesis: Increasing Wind Turbine Efficiency

Name of the student: TUKA FATTAL

Exam date: 06 September 2018

Approval of the Graduate School of Natural and Applied Sciences.

Prof. Dr. Ahment Necmeddin YAZICI

Director

I certify that this thesis satisfies all the requirements as a thesis for the degree of Master of Science.

Asst. Prof. Dr. M. Orkun ÖĞÜCÜ

Head of Department

This is to certify that we have read this thesis and that in our consensus opinion it is fully adequate, in scope and quality, as a thesis for the degree of Master of Science.
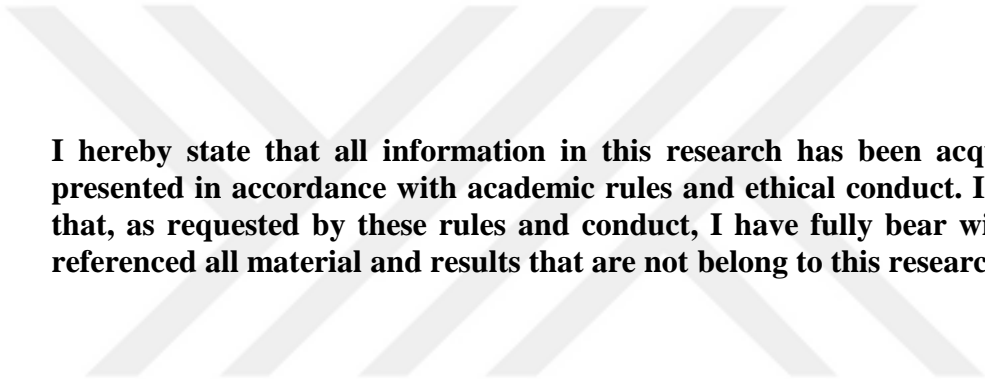
Supervisor: Prof. Dr. İbrahim H. GÜZELBEY

Examining Committee Members

Prof. Dr. İbrahim H. GÜZELBEY

Asst. Prof. Dr. Mehmet HANİFİ DOĞRU

Assoc. Prof. Dr. Selçuk MISTLKOĞLU

I hereby state that all information in this research has been acquired and presented in accordance with academic rules and ethical conduct. I also state that, as requested by these rules and conduct, I have fully bear witness and referenced all material and results that are not belong to this research.

Tuka FATTAL

ABSTRACT

INCREASING WIND TURBINE EFFICIENCY

FATTAL, Tuka
M.Sc. in Aircraft and Aerospace Eng.
Supervisor: Prof. Dr. İbrahim H. GÜZELBEY

September 2018
71 pages

Renewable energy technology considers as alternative solutions to reduce the carbon emission and global warming potential in the world. In the renewable energy, wind and solar cell power are the best techniques to produce the power. But the efficiency of the systems is low compared to the conventional method. The purpose of this research is to develop a smart model of a wind blade which enabling the blade to change its area according to wind velocity in order to achieve best angle of attack of each, this concept is against increasing wind size to increase wind efficiency, however, other barriers of maintenance and the dramatically increases of cost are apparent when we mention increasing wind turbine size. The smart blade could be the alternative solution of the size increasing. Two different smart blade models have been analyzed at different wind velocity and best angle of attack discovered where efficiency is perfect.

Keywords: wind turbine design, wind turbine structure, efficiency, smart blade, aerodynamics, renewable energy, energy sources, aerodynamic efficiency.

ÖZET

ARTAN RÜZGAR TÜRBİNİ VERİMLİLİĞİ

FATTAL, Tuka
Yüksek Lisans Tezi, Uçak ve Uzay Müh Tez
Yöneticisi: Prof. Dr. İbrahim H. GÜZELBEY

Eylül 2018
71 sayfa

Yenilenebilir enerji teknolojisi, dünyada karbon emisyonu ve küresel ısınma potansiyelini azaltmak için alternatif çözümlerden biridir. Yenilenebilir enerji üretiminde rüzgar ve güneş pili en iyi tekniklerdir. Ancak, sistemlerin verimliliği geleneksel yöntemle karşılaştırıldığında daha düşüktür. Bu araştırmanın amacı, bir rüzgar türbini kanadının akıllı bir tasarımla geliştirilerek kanatların rüzgarın yönüne göre kendini ayarlaması böylece en verimli açıyı yakalayarak rüzgarın şiddeti yerine verimliliğini elde etmesini sağlamaktır. Bu yöntem rüzgar türbinlerinin ebatlarında büyüklüğü ve onların getirdiği tamirat ve tadilat masraflarının etkili bir şekilde en aza indirgenmesine yönelik te çözümler sunuyor. Bu akıllı kanatlar türbinlerde ebat büyüklüğüne yönelik alternatif bir çözüm getiriyor. Farklı şiddette rüzgarlara karşı en etkin açıyı elde edip en üst düzeyde verimliliği keşfeden iki ayrı akıllı kanat tasarımı analiz edildi.

Anahtar Kelimeler: rüzgar türbini tasarımı, rüzgar türbini yapısı, verimlilik, akıllı türbin kanatları, aerodinamik, yenilenebilir enerji, enerji kaynakları, aerodinamik verimlilik.

ACKNOWLEDGEMENTS

I would like to address my deepest thanks to my supervisor Pro. Dr. Ibrahim H. Güzelbey for his support, advice, encouragements and insight me during the implementation of the research.

TABLE OF CONTENT

TABLE OF TABLES

LIST OF FIGURES

xv

LIST OF SYMBOLS

A	Swept area
WT	Wind turbine
RE	Renewable energy
CL	Lift coefficient
CD	Drag coefficient
β	Angle of attack
α	Angle between Wind turbine blade parts
AR	Aspect ratio
ρ	Air density
V_i	Wind velocity
P	Power produced
C_p	Power coefficient
HAWT	Horizontal axis wind turbine
VAWT	Vertical axis wind turbine
NREL	National Renewable Energy Laboratory
M	Aerodynamic moment
C_l	Lift coefficient
C_d	Drag coefficient
Re	Reynolds number
b	blade length
γ	Complementary Angle
WF	Wind Flow
FF	Front Face
NACA	National Advisory Committee for Aeronautics

CHAPTER 1

INTRODUCTION

1.1 Thesis Outline

This research is organized into six chapters, where chapter one concerns with clarifying the motivation of this research and gives a brief background on renewable energy sources; summarize the wind turbine history and how humanity developed investment in wind energy. In the second chapter is a literature review of increasing wind turbine efficiency attempts and have a close look on similar studies and researches on wind turbine smart presented and discussed, In the third chapter types of wind turbine explained and main components demonstrated. The fourth chapter introduces the work approach and how we decide the optimum angle of attack for the first smart blade model while in the second smart blade model we negotiate the concept of change the blade surface and how it affects the WT efficiency. After that, the fifth chapter presents the results, discusses the increasing efficiency problem from a new overview, the sixth chapter concludes the research of this thesis and gives few directives for any possible future work, the last chapter we highlight the future work according to this research.

1.2 Motivation

Wind turbine is considering as an important renewable energy sources in the new century, the continues consumable of power sources by humanity will lead to a lack of available sources for the new generations in addition to the harm caused to the environment, however, humanity should search for new sources able to cover the increasing of demand of power. The renewable energy is one of the alternative sources of energy which naturally occurring, the theoretically inexhaustible source of energy. Man tried to exploit the natural energy sources a thousand years before Christ, later on, people depend on other energy sources, but due to the uncontrolled consuming of these resources all of these resources will be finished, in another word during the upcoming hundreds years humanity will not be able to utilize any of these sources, however, people go back to

history and took lessons which led them to depend on the renewable energy instead of relay on the consumable energy resources. Wind energy has been exploited to produce energy long time ago, using windmills and later wind turbines which is the modern face of the windmills, but people stay unable to utilize more than 49% of kinetic energy of the wind due to many factors listed in the research. Using new approach such as smart blade model can give some additional options to increase power extracted from wind, by the continuous exploitation of wind energy at high and low limits which are 23 m/sec and 3 m/sec. While other attempts were constraining on raising tower length, rotor size or using a smart rotor system and that caused a huge increase in cost.

1.3 Most Known Types of RE

1. Solar energy [1] [2].

2. Wind power [3] [4].

3. Hydroelectric energy [5].

4. Biomass [6].

5. Hydrogen and fuel cells [7].

6. Other forms of energy [8].

1.4 Wind Turbine History

Humanity started utilizing wind energy to propel boats along the Nile River as early as 5,000 BC [9]. Old nations used windmills to grind corn, grind flour, and pump water. The first modern wind turbine generating electricity as it known nowadays was established in July 1887 by Scottish Academic [10].

Figure 1. 1. The ancient Egyptians around 2500 BC. sailing ships in the sea [9]
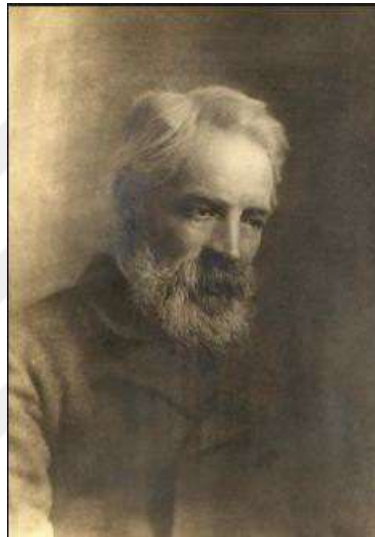
Figure 1.2. Professor James Blyth MA [11]

Later a Danish scientist improved an electricity-generating wind turbine and later discover how to supply a steady stream of power from the wind turbine by utilize of a regulator [11]. Early with the starting of the twenty century the first horizontal-axis wind turbine as we use today is built [12]. During the Second World War small wind turbines are used on German. The huge wind turbines improved according to these efforts set several world records for dimensions and power outcome [13] [14].
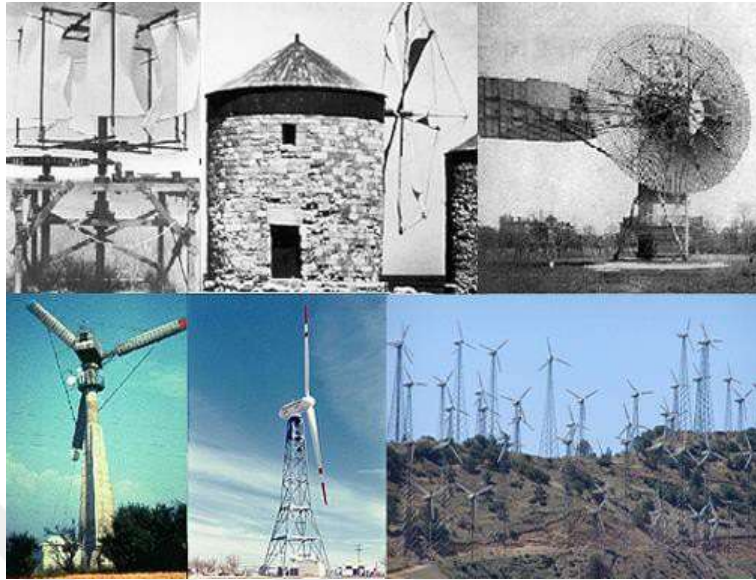
Figure 1.3. Early stages of wind energy exploitation [15]

CHAPTER 2

LITERATURE REVIEW

2.1 Introduction

This chapter will cover some humanity attempts to increase wind turbine efficiency because wind energy is considering as the best source of clean energy in the modern decade. Wind is not like the sun it is available all time in all places, in another hand, the variability of wind causes severe constraints on the design of wind machines, which reduces its effective capture of available wind energy. The race of achieving the best performance of WT currently is the basic concern of the developing nations. Soon ordinary energy sources would not be available anymore, however, providing the required amount of energy would be a big challenge facing governments and population.

2.2 Increase wind turbine blade efficiency attempts

If we look at wind turbine before ten years ago and a close look on it nowadays we can recognize the dramatically increase of development of it in the rotors, controls, electronics, and gearboxes — but the advancing technology used in wind power production has always aimed for the same goal: making wind power a better choice for power generation. Hence, improving wind turbine efficiency and reduce cost.

Increasing wind turbine efficiency can be achieved by different concepts, such as constraining on developing the gearbox, increase the rotor size, examine intelligent control systems, blades number, size and shapes and pitches [15]. Ordinary wind turbine blades subjected to many attempts to develop the structural design, manufacturing materials and developing the rotor control system of the blade. In 2008, a scientific research conducted a comparing between flat and curved blade and how curved blades give better efficiency because curved blade has air flowing around the blade with the air moving over the curved top faster than it does under the flat side of the blade which create a lower pressure area on top, hence, as a result, is subjected to aerodynamic lifting forces

which create movement. These lifting forces are always perpendicular to the curved blade's upper surface which led to the blade to move rotating around the central hub. The faster the wind blows, the more lift would produce on the blade, and therefore the faster the rotation. The advantages of a curved rotor blade compared to a flat blade is that lift forces enable the blade tips of a wind turbine to move faster than the wind is moving to generate more power and higher efficiencies. As aresult, lift based wind turbine blades are becoming more common now. In 2014 some scientific papers addressed a problem of poor performance of small WT which working at low wind velocity due to laminar separation and laminar separation bubbles on the blades, this can be defined due to the low Reynolds number (Re) as a result of low wind velocity and small rotor size, however, the utilize of specially designed low Re airfoil permits start up at lower wind velocity, increasing the start-up torque and thus improving the overall performance of the WT [16]. Other attempts seek to study and understand the turbulent loading effect on wind turbine performance, In the past, the effect of turbulence has been considered in many domains such as heat transfer, combustion, and aerodynamics. The study of turbulence of aerodynamics phenomena related to wind turbines is rapidly becoming one of the major issues of interest within the wind energy community, this research used experimental approaches to study the influence of turbulent flow on the performance of the WT and loading of a scale-representation of a three-bladed wind turbine. A miniature turbine with a rotor diameter of 384mm was developed and tested within a wind tunnel of 0.9m×0.9m cross-section. To predict the performance of the wind turbine, the lift and drag coefficients of a 2-D foil have been measured over a range of Reynolds numbers and angle of incidences. The measurements have been carried out downstream of the turbulent flows which were simulated in the wind tunnel to be the representative of an atmospheric boundary layer with turbulent intensities ranging from 0.5% to 23% and length scales ranging from zero to 210mm. This range of turbulence characteristics was developed using vortex generators, barrier wall and bed-mounted cubes and the grid turbulence generator. It was observed that when the vortex generators with the barrier wall and the groups of cubes generated the background air flow, the level of turbulent intensity was up to 23% at 150mm from the ground and 6% at 450mm with a range of integral length scales from 210mm at the level of 150mm to 150mm at the level of 450mm. Meanwhile,

the grid turbulence generator could not sustain greater than a 35mm length scale; however, it can maintain a higher level for the turbulent intensity (16%) at a cross section five mesh sizes downstream [17].
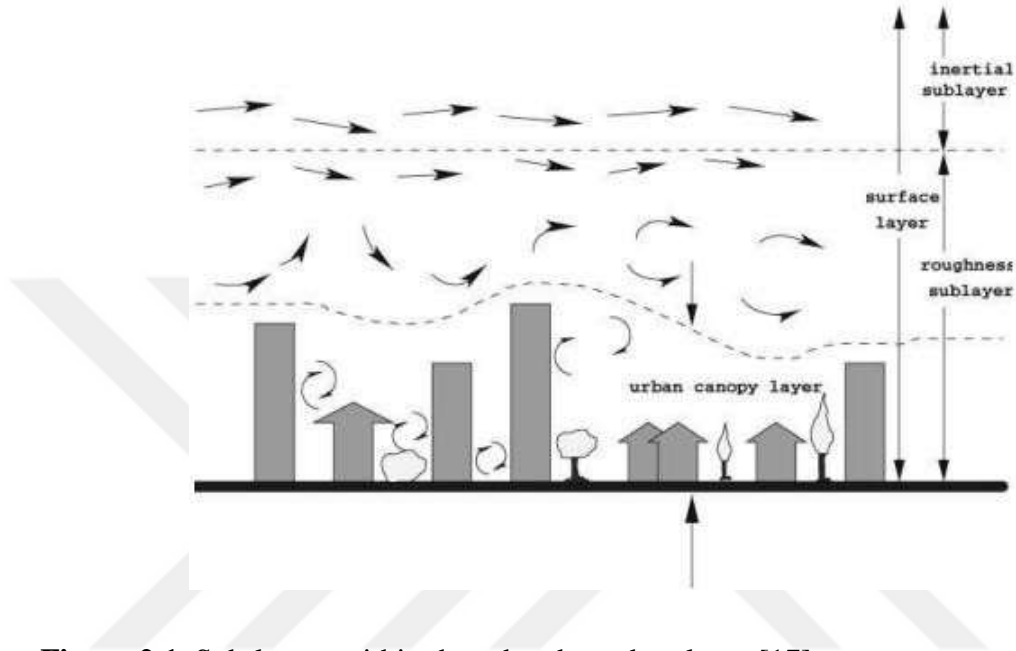
Figure 2.1. Sub-layers within the urban boundary layer [17].

In Germany 2014, 19 wind turbines in four farms subjected to non-convex efficiency analysis to determine losses, then in a second stage regression, they adapt the linear regression results of Kneip, Simar, and Wilson (2014) to explain electricity losses by means of a bias-corrected truncated regression analysis. The results show that electricity losses amount to 27% of the maximal producible electricity. Most of these losses are from changing wind conditions, while 6% are from turbine errors [18]. Other attempts seek to reduce the establishment cost of the wind turbine to increase the benefit of the wind turbine. However, in 2001 the tallest wind turbine tower with more than 65 m, but the cost was huge, as an alternative solution to this huge cost an attempt in 2002 and 2003 started to build the WT in the construction site, and still under study but to build a WT with a tower of 100 m to increase wind turbine efficiency [19]. Later new methodology of developing wind turbine blades created which is modeling the smart structure of wind turbine, this study highlighted how developed load control techniques has induced the interest in aerodynamic control systems with built-in intelligence on the blades, this study

shows the structure of blade vibration protection using piezoelectric materials is suggested. The blades modeling is completed, the embedded construction of piezoelectric materials is designed, the analysis of deformation displacement and stress of piezoelectric material which proved that the glass fiber composite with piezoelectric materials can be used for the blades active vibration control with Algor software. Blade modeling and finite element analysis of piezoelectric structures are contributed to analyzing the problem of wind turbine blades aeroelastic and lay a foundation for blades stability [20].

CHAPTER 3

WIND TURBINE TYPES AND COMPONENTS

3.1 Introduction

This chapter explains the main parts of WT, the role of each portion in producing power, converting wind kinetic energy to electric power for daily basis. Constraining on wind turbine blades design, affecting the wind turbine performance as the developing of the wind turbine blade ordinary airfoil to be a smart blade. In another hand, this chapter explains the main differences between windmill and wind turbine.

3.2 Wind Turbine Overview

The main goal of designing a wind turbine and designer is to maximize the aerodynamic efficiency or power extracted from wind, the places of fixing the wind turbine [21]. Wind turbine is a machine which is catching wind kinetic energy to produce electricity by converting this energy to rotational energy, wind turbine is working by opposite of fan which using electricity to work, offshore and onshore wind turbines have the same work principles, however the wind energy rotates wind blades around the rotor which is connected to the main shaft "low-speed shaft" as the produced rotation isn't enough to produce power. The drivetrain contains the gears which responsible for increasing the rotational speed "high- speed shaft" this shaft is connected to a generator which creates electricity. The Planform is with the span of 9.8 m and an aspect ratio of 6.8. The lift to drag ratio (glide ratio) has been estimated to be about five. According to Rankine-Froude theory, the generated power (P) by a known wind turbine calculated by the following equation [22]:

$$P = \frac{1}{2} \rho A V_i^2 C_p$$

(3.1)

Where ρ is air density, sweep area is, wind velocity is V and Power coefficient is C_p which is constant and equal to 0.4[23].

3.3 Wind Turbine and Windmill

The main difference between WT and windmills are utilized mechanical energy for some purposes like grain grid or pump water directly, while WT convert this mechanical energy to electrical energy [22] [24].

a. Wind turbine [9]   b. Windmills [9]

Figure 3. 1. Wind turbine & windmill

3.4 Wind turbine classification

In general, WT can be classified in two main types horizontal axis WT and vertical axis WT, HAWT called like this. Because its shaft is parallel to ground while VAWT shaft is perpendicular to ground, both types have advantages and disadvantages, any way HAWT is still more common and there are many designs of it available in the commercial markets for many reasons can be listed later [25].

a. HAWT [25]   b. VAWT [20]

Figure 3.2. Wind turbine classified according to main shaft

3.5 Wind turbine components

The ordinary wind turbine as it is known nowadays consisting of 16 parts, each of it has a precise and clear rule with power production process [26] [27].

Table 3.1. Wind turbine components

1. Nacelle	9. Wind vane
2. Blade	10. Anemometer
3. Hub	11. Low speed shaft
4. Pitch system	12. Break
5. Main shaft	13. Yaw drive
6. Gear box	14. Yaw motor
7. Generator	15. Tower
8. Controller	16. Rotor
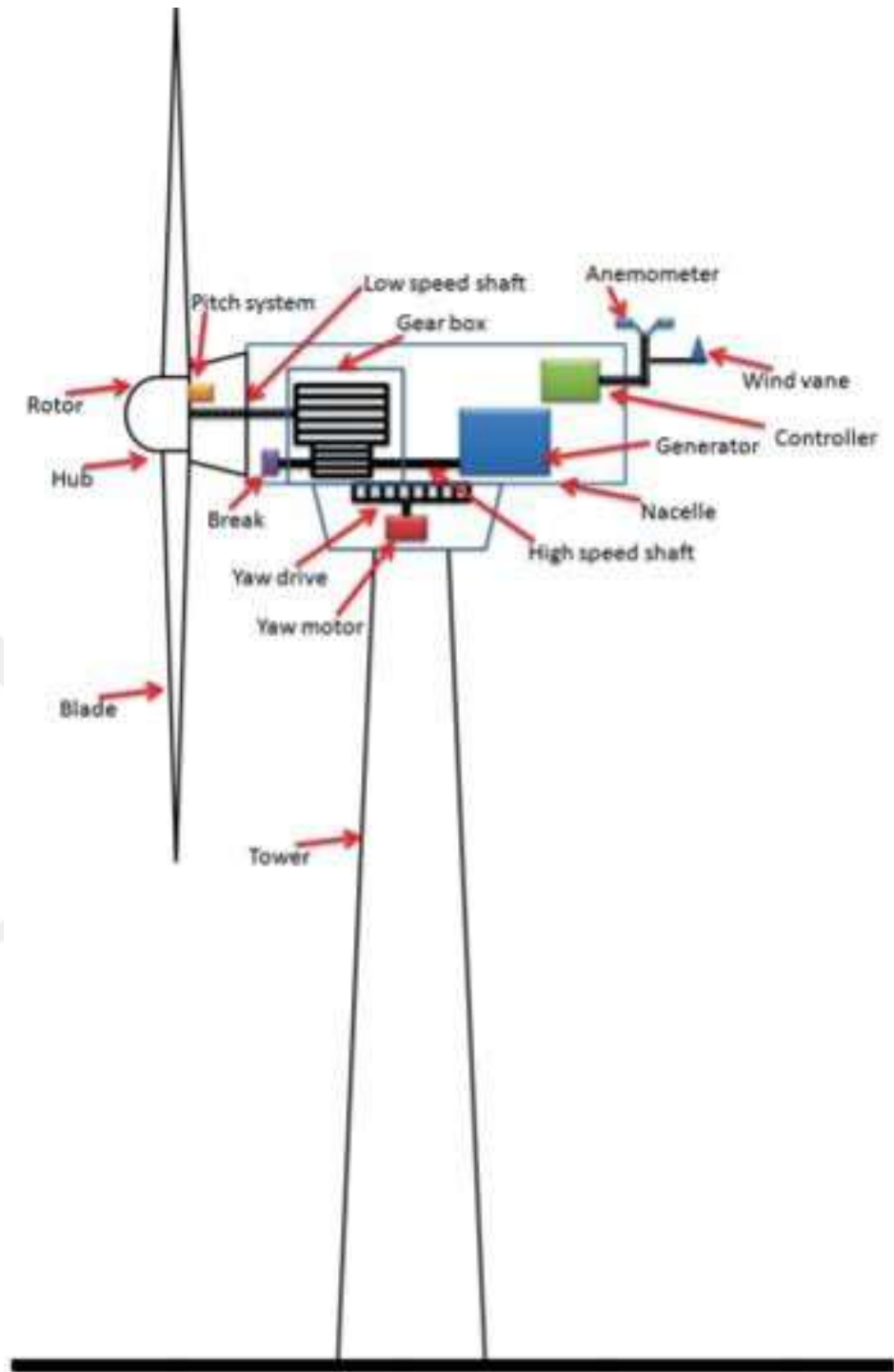
Figure 3.3. Wind turbine components [23]

3.5.1 Nacelle

The nacelle is the part that located at the top of the tower and connected to the rotor as well as it supports additional parts such as the generator and drivetrain, the nacelle is really big while it is enough for a helicopter to land on, the rotor nacelle converting the captured energy kinetic energy of wind to rotational energy [26]. The rear of the

main shaft is connected to the slow-rotating side of the gearbox while the main shaft supports the rotor. The electrical generator became after the gearbox, in the front of the generator there is a big desk which has the ability to keep the turbine in stopped position while the transformer of each produced electricity phase produced usually based at the back of the nacelle, in generic three-phased electrical power generated, which should be then transformed to higher voltage (HV) of the gird, the power cable conveys generated electricity from the generator to the grids. The cable is in the tower. As the nacelle yaws, the cable twists to face the wind direction. The control system counts the number of cable twists to ensure that the cable is kept within defined and safe limits [28].

Figure 3.4. Nacelle in the wind turbine components [23]

3.5.2 Hub

Most modern wind turbines are utilizing pitch-controlled variable-speed generators which means that the pitch angle of the blades are changed to optimize the produced power. Hub is connecting blades to the main shafts and at the end to the rest of the drive train. Hub must hold out all the loads generated by the blades. Hubs are generally made of steel, either welded or cast [28].

Figure 3.5. Hub in the wind turbine [23]

3.5.3 Blades

Blades are the parts which catch the kinetic energy of the wind and transfer it to rotational energy, blades are fixed on a specific bearing, which enable the blades to pitch "to change their angle relative to the hub while they are still in the rotor plane". The angle of attack of the blades (relative of the wind) can accordingly be optimized, so blades make the maximum lift for different wind velocity without stalling. Blades are feathered to maintain the rated power when wind velocity gets high, while fast pitching of the blades to zero degrees provides an effective means to stop. Early wind turbine blade depends on airplane wing airfoil, same aerodynamics forces control both blades work [13]. Manufacturing WT blades forming 15-20 % of the total cost, the aerodynamics profiles of WT blades have a crucial influence of WT [20].

The blade has an airfoil shape different along the blade length from root up to the tip, and the most common wind turbine has a blade with a length of 16 - 19 meter with three blades. Early blades were flat which were very common, flat blades were used in the windmills, when wind turbine design developed, blade shape change, and

curved blades appear. The curved blades are very similar to airplane wings where lifting forces cause blades rotation, as it causing airplane taking off [29]. Similar principles control both systems, lift and drag forces, different pressure on both faces of the blade, however, we can say that the wind turbine blade simulate airplane wing [28] [30]. For purposes of efficiency, control, fuss, and aesthetics the modernistic wind turbine market is dominated by the horizontally mounted three blade designs, with the utilize of yaw and pitch, for survive and work under different wind velocities ability. An international supply chain has evolved around this design, which is now the industry leader and will remain so soon. Usually manufacturers aiming greater cost efficiency have exploited the ability to scale the design, while the latest models
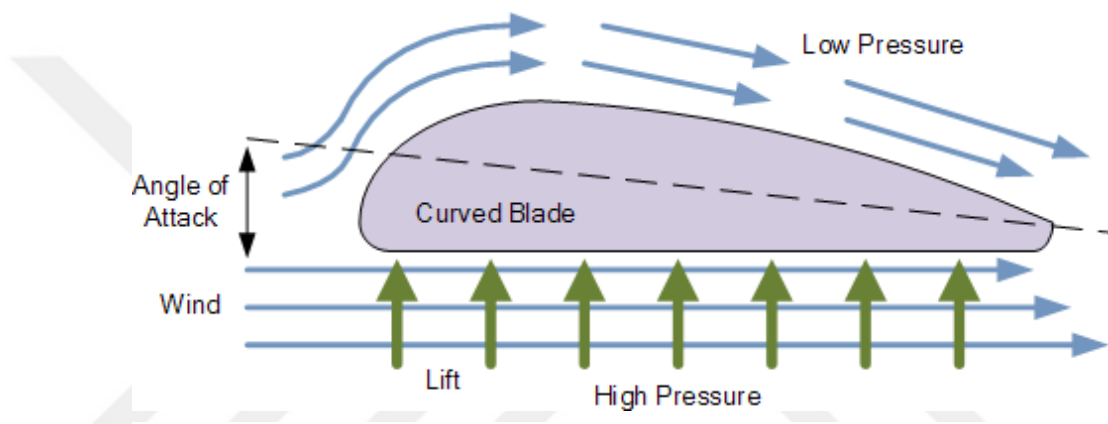
reaching 164 m in diameter [23].

Figure 3.6. Wind turbine blade airfoil [26]
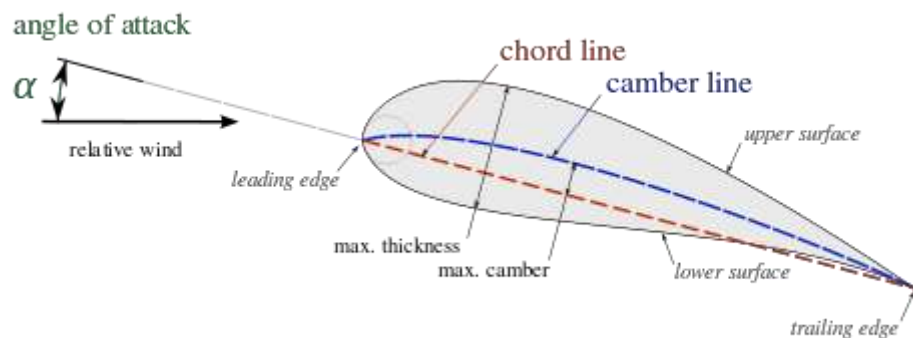
Figure 3.7. Wind turbine blade airfoil [27] [28]

15

The main purpose of the curved surface is to reduce drag forces which caused by the friction of air with blade surface, the drag force is perpendicular to lift force with the same direction of air flow [31] [32].
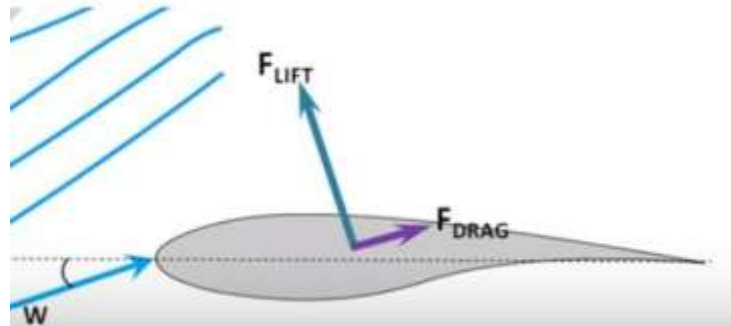
Figure 3.8. Lift & drag forces [31]

Number of blades has direct influence on wind turbine efficiency because when number of wind turbine blades increases aerodynamic efficiency increases but in diminishing manner, depending on the development of the wind turbine design history when we move from two blades wind turbine to three blades wind turbine efficiency increased by 3% but when we moved from three blades wind turbine to four blades wind turbine efficiency gain is marginal increase estimated by 0.5% only while cost is increased dramatically, and the chemical design of the blades becomes a difficult

affair with more blades [30] [33] .

Figure 3.9 Blade with two, three and four blades [24]

That is why we can see that the wind turbine with the three blades is more common nowadays. Blades must be thinner to be aerodynamically efficient, in some manner root may not withstand bending stress induced due to axial loads for that wind turbine with three blades accommodate a thicker root are used commonly. In other hand, the next big factor affecting the performance of the wind turbine is shape and orientation of blade cross-section a moving machine experiences fluid flow at different velocity than the actual velocity and it's called the relative or apparent velocity (W) and it is equal to the difference between the actual flow velocity (wind speed V) and blade velocity (U)) as the following equation demonstrate [34].

$$\vec{W} = \vec{V} - \vec{U}$$
(3.2)

If this is the real flow velocity a rotating blade will experience an apparent of this at a particular cross section, a deep look at the wind turbine will detect that it is having an airfoil cross-section from root to tip, the driving force of the wind turbine is lift force of wind turbine is lift force generated win-win flows over such airfoil, the lift forces are perpendicular to the apparent velocity.

In general, lift force increases with angle of attack. Along with that the drag force increases well tangential component of lift force supports blade rotation drag force opposes it so a wind turbine can give maximum performance when lift to drag ratio is maximum [35].
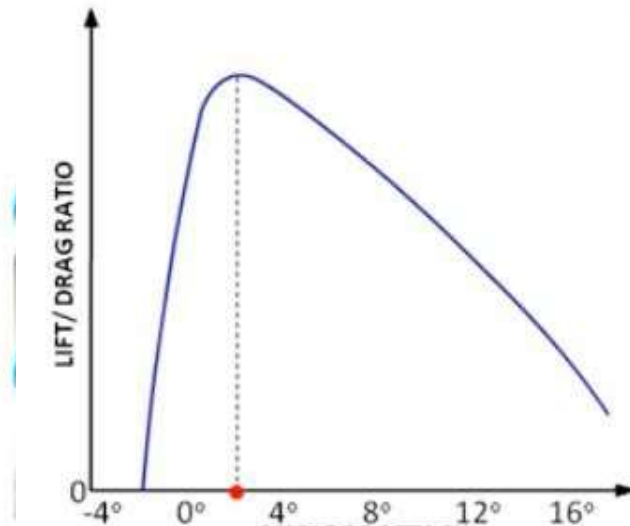
Figure 3.10 The relation between angle of attack and lift to drag ratio [34]

The red point in fig3.10 called the optimum angle of attack, airfoil cross-section are aligned in a way to act at this optimum angle of attack "even though flow velocity is uniform along length of the blade", blade velocity increases linearly as we move to tip, so angle a magnitude of relative velocity varies along length of the blade, the apparent velocity becomes more aligned to chord direction as we moved to tip so there must be a continuous twist and blade so that at every airfoil cross-section angle of attack is optimum. When condition can change at any time it is possible to rotate WT blades in its own axis to achieve optimum of attack with varying wind condition, this is known as pitching of blades a clever algorithm which uses when condition and characteristics of wind turbine as input governs the pitch angle [36]. Blade length affecting WT performance [37], according to equation (3.1) a longer blade will favor the power extraction P α L2. But with increase in blade length deflection of blade tip due to axial wind force also increases, however, unstudied or blind increases in length of the blade may lead to dangerous situation collision of blade and tower, with increases in blade length tip velocity increases, noise produced by turbine is strong function of tip velocity, however, there is a limit on blade length shouldn't passed "over defection of blade problem of noise". The relationship between the produced moment and wind turbine performance belong to lift force, as mentioned above as the lift to drag ratio bigger the performance of the wind increased [38].

$$\text{Lift to drag ratio} = \frac{c_l}{c_d}$$

3.5.4 Pitch System

The pitching system rule is rotating the blades around its own axis in such a way to lessen air resistance in another word "feathers the blade above the rated wind speed", the controller decides how much the actuators need to turn the blades while the relative angle between the incoming wind and blade chord should be controlled by a controller hence, the pitch system applies the controller's commands and feathers the blades.

Figure 3.11 Pitch System in the wind turbine [14]

Ancient wind turbine has blades connected directly to the hub with a fixed angle, these turbines haven't pitch system, however, if the wind flows were strong this blades would stall as the angle of attack would be increased by the increase of wind speed, this had a pros effect on the survivability of the WT and contributing to protect the WT components, such as blade and tower [39]. Fixed angle of attack reduces the amount of generated power; however, the turbine's maximum rated production could only reach within a narrow range of wind speed install regulated WT. Fortunately modern WT has a pitching system because its help to utilize wind energy when its blow in lower speed and increases the range of wind speed in which the rated power is captured. When wind speed becomes higher, the blades pitch to smaller angle of attack and rated power is maintained, this enabling WT to survive in the harsh conditions, meanwhile, the produced power increased [40].

Figure 3.12 Pitch System in the wind turbine [14]

3.5.5 Main Shaft

Wind turbines as it's known recently including low-speed shaft and high-speed shaft, the main shaft is a massive part usually built forged or cast iron while the new industrial start to use carbon-fiber-reinforced polymer (CFRP) to reduce the shaft weight and saving several tons in the complete nacelle. However, the main shaft is the low-speed shaft which drives the high-speed shaft, in other hand, the latest is connected to the gearbox and transmit the mechanical power of the rotor to the generator [41].

Main shaft has paramount functions as it supports the rotor (hub & blades), as well as transmits the rotary motion of the rotor torque moments to the gearbox and /or generator [42]. Thrust forces are taken by the shaft and transmitted to the nacelle and to the top of the tower of the WT [43].
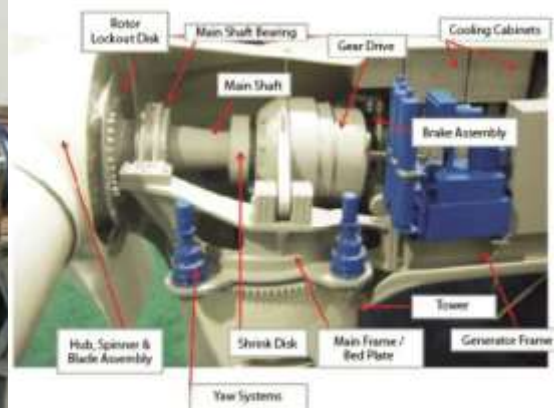
ι.   Main shaft of the WT manufacturing   b.   Main shaft location in the WT

Figure 3.13 Main shaft [14]

3.5.6 Gearbox

The gearbox connected the main shaft (low-speed shaft) to the high-speed shaft, the main role of the gearbox is maximizing the produced rotation speed "rotational speed caused by blade rotation isn't enough to produce any electricity power", such an example a wind turbine of 1MW, the rotational speed is about 20 (rpm) which means that the gearbox able to increase the rotational rotor by a ratio of about 90 times to get the rotational speed of high-speed shaft to reach about 1800 (rpm), the most common wind turbine around the world which considered as large turbines are wind turbines 5 MW while the gearbox ration and high-speed shaft rpm respectively are around 12.1, 97 and 1173.7 (rpm).

Figure 3.14 Gearbox connecting low-speed shaft to high-speed shaft[14]

A wind turbine may need a gear system depending on its generator type. Some wind turbines do not need a gearbox and they are gearless (direct drivetrain). Gearbox design in a wind turbine is tightly linked to the choice of generator. Electric generators need high rotational speed input [44]. However, the rotor of a wind turbine is rotating relatively slow. Hence, a gearbox system is needed to raise the rotational speed of the input torque. The low-speed shaft (main shaft) is connected to the hub and delivers the torque to the gearbox. The gear systems, which consist of several types of gears, increase the rotational velocity about 100–200 times for MW turbines (depending on the type and scale of the turbine) [45]. The high-speed shaft is connected to the generator. The main shaft speed is dependent on the blade tip speed and the length of the blades. Hence, longer blades result in slower rotation of the main shaft as it is

needed to keep the tip velocity subsonic. The power is a multiplication of rotational velocity and torque. When a gearbox increases the rotational speed, it simultaneously decreases the torque[46][47].
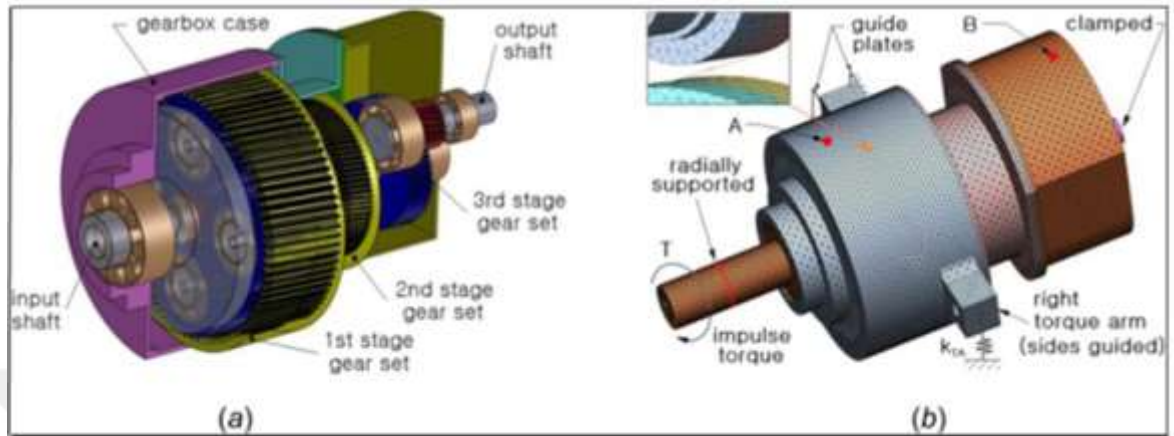
Figure 3.15 Wind turbine gearbox components [14]

3.5.7 Generator

The generator is considering as the main electrical portion of the WT that produces 60-Hz alternating current (AC) electricity, and it is usually an off-the-shelf induction generator [29]. Relatively high rotational speed is required by most generators to produce electricity. As mentioned previously there are gearless wind turbines, in which the idea is to remove the gears, and the turbines operate with "direct-drive" generators that operate at lower rotational speeds and do not need gearboxes [48]. Normally the gearbox is a costly (and heavy) portion of the wind turbine and forming an extra weight in the nacelle while removing it can have some advantages. However, more research is needed to investigate and develop a mature gearless turbine [49].

3.5.8 Control system

The control system is utilized to improve the functionality of a WT, while the other basic roles of it are to increase the power production and limits the loads on the structural parts, during the last ten years WT manufacturing apply active control system to achieve the best performance. The control system consists of a few parts which continuously monitor the condition of the wind turbine and collect statistics of operation from sensors [29]. However, it is worth to mention that the turbine rotor is

straight into the coming wind. Any perversion results in a reduction of energy, the yaw system turns the nacelle and the rotor based on received information from the central controller. As mentioned previously, the pitch system feathers the blades to adjust the angle of attack which designer try to achieve with each wind speed to secure the maximum benefit from the kinetic energy of the wind, the controller monitors and adjusts the angle of attack based on the wind direction and wind speed measurements [50]. This technology offers the path for new control concepts like feedforward control and model predictive control to increase the power production and to reduce loads of wind turbines [51].

CHAPTER 4

SMART BLADE MODELS

4.1 Introduction

This chapter explains the main reasons of wind turbine collapse; however, this study will have explained how the concept of smart blade is able to increase wind turbine efficiency at high speeds of wind where normally WT acting as a wall or can be collapsed in other cases. To achieve a theoretical evidence of improving wind turbine work conditions two types of the smart blade "using Solidworks software" have been drawn and examined at a different angle of attacks while wind velocity took different values, the study implemented at wind speeds of 5 m/sec, 8 m/sec, and 23 m/s. This research discussing the two scenarios. The smart blade has a changeable airfoil which give the blade the ability to change the contact surface with the wind according to wind velocity. All loads on both surfaces of the blade have been considered in the study, the purpose of the study is searching for the best angle of attack for the assumed wind velocity which is accompanied by a certain value of the angle between both blade parts to prove that each wind speed has its own optimum angle of attack besides a special angle between the two parts of the blade where the efficiency of the turbine is maximum. The airfoil of A NACA 4705 has been used in the modeling.

4.2 Wind Turbine Collapse

Excessive winds strictly endanger structural integrity of wind turbines, these extremist winds influence wind turbine blades because of its speed and larger change of wind direction which causes in sometimes tower collapse and blade fracture. When wind speeds exceed 25 m/s blade feather position and a revolving rotor should be stopped aerodynamically but this system for some reasons didn't stop the rotation of the blade which causes blade collapse [52], however, blades able to collapse at 71.5 m/s. Tower of the wind turbine can be collapsed at 59.8 m/s while the typical model survival wind speed of 70 m/s. Nacelle has a number of systems which if they fail, can cause blade destroyed [53].

The lifespan of the wind turbine typically is 20 years, some of wind turbine farms couldn't work until the typical work period due to the reasons listed above.

4.3 Smart Blade Models

4.3.1 First smart blade model

The first model is a smart blade with changeable surface able to take different positions according to wind velocity. The blade is consisting of two parts fixed to each other from the middle with special rubber joints, this model shows the ability of the smart blade wind turbine to cross over the cutting of the torque when velocity achieved the maximum value where wind turbine still able to produce torque. Blade properties explained in table 4.1.

Table 4.1 Wind turbine blade properties

Blade	Dimensions
Blade length	mm
Blade width	mm
Blade material	Metal
Front surface area	mm^2
Back surface area	mm^2
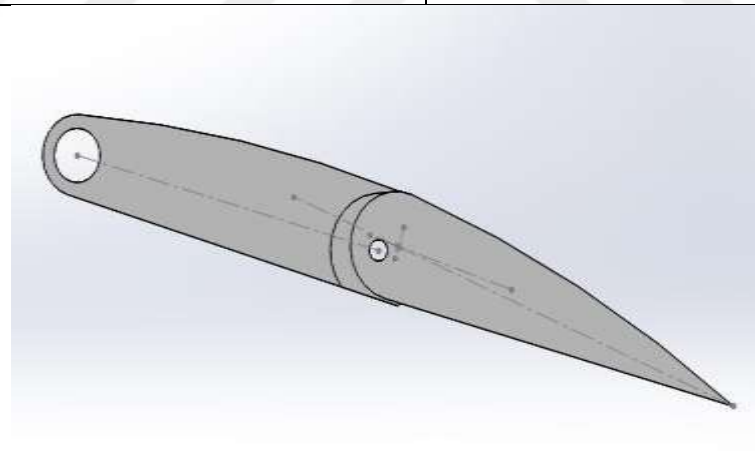
Figure 4.1 First smart model of wind turbine blade

Let's define study parameters, α is the angle between the both parts of the blade this angle will take different values in another word, we are going to change this angle until we achieve the best outcome moment M, this torque will be responsible of rotating the blade, hence, more of torque means more of electricity. The following values of **α** will be tested α = (7°, 11°, 15°, 17.5°, 20°) fig a.4.2. While, β is the angle of attack

25

which means the angle between.the relative wind velocity and blade cord fig b.4.2. During our experiment we will give β different values as the following β = (10°, 13°, 15°, 16°, 17°), as a first step we will fix α at 7° which consider the zero point for our study and changing β according to the previous values, this step will enabling us from determining the best angle of attack for wind speed of 5 m/s, then we will start to repeat the study but with fixed β and changing α to previous values. When we start applying the flow pressures on both faces created with different values, however values and pressure distribution are explained in figures and table listed for each case of the study. Area of both faces isn't fixed because the front face is curved while the back face isn't, we can recognize that each part of the blade area subjected to different values of pressure and that what appears in pressure analyzing. During the calculation we used the percentage of each area subjected to certain pressure as % the measurement unit is mm^2. Then the forces (Kg) applied on each area calculated using equation (4.1) where A (mm^2) is the area affected by a certain amount of pressure according to the analysis, applied forced on the front face have been gathered and same for forces applied on the back face, the difference between the two forces used to determine F_a the force affecting the blade, this force and according to applied angle of attack will support our calculation to discover F the force which cause the moment and calculated according to equation (4.2), where γ in the complementary angle of the incident angle, however, the last produced moment calculated according to equation (5.3) where b is the length of rotating arm (the space defined as the distance between the rotating center and the middle of the blade length) b= $320*10^{-3}$ m.

$$Fa = P*A \qquad\qquad (4.1)$$

$$F = Fa * \cos\gamma \qquad\qquad (4.2)$$

$$M = F * b \qquad\qquad (4.3)$$
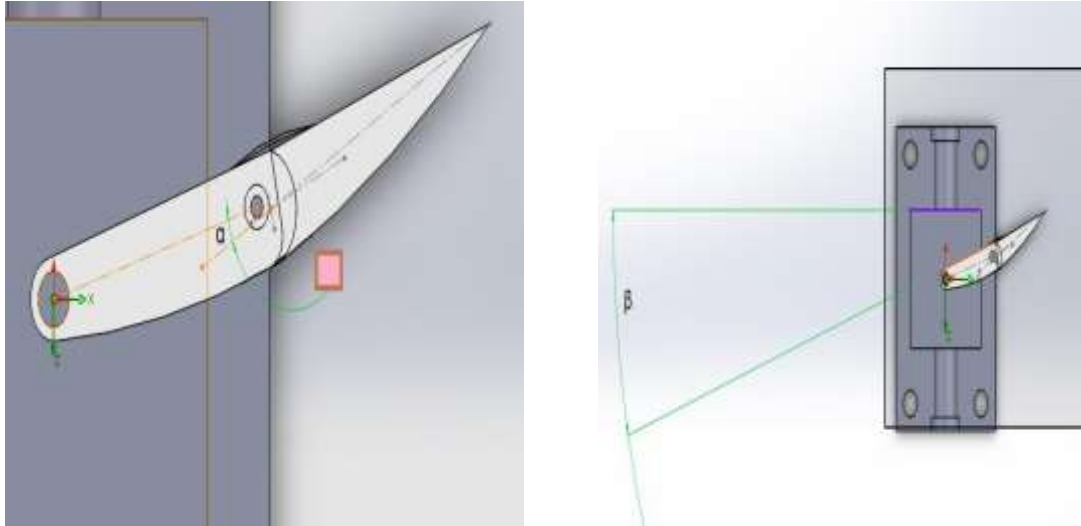
a. The angle between the both parts of the blade   b. The angle of attack

Figure 4.2 Angle between blade parts & angle of attack

During the experiments and while we implement our calculation we used the global units, pressure by Pa, forces by Newton, torque N.M, velocity M/S and lengths by m.

4.3.1.1 Fixed angle between blade parts

İn the first case we fixed the angle between the two blades at $\alpha = 7°$ which consider the zero angle between both parts because we negotiate a concept of curved blade with an angle between the two parts, and move the whole blade in many different values of angle of attack as the following $\beta = (10°,13°,15°,16°,17°,20°,25°,30°,35°,45°)$, during this test we will try to discover the ideal angle of attack to move to the next phase of the experiment which will test different angle between the two blades according to the optimum angle of attack, in other word, from the first test we will determine best angle of attack for the 7° which is the basic state between the two blade parts then we will try to determine the best angle between both parts of the blade depending on the discovered the best angle of attack.

Table 4.2 The produced forces when α = 7°, β = 10° & γ=80°

Blade Faces	Pressure / Pa	Pressure Kg/mm^2	Area mm^2	Area %	Area subjected to pressure /mm^2	Force / Kg
Front face	101336.13	0.010333245	48463.9	40	19385.54	200.3155377
	101331.53	0.010332776	48463.9	20	9692.77	100.1532223
	101326.33	0.010332246	48463.9	20	9692.77	100.1480828
	101322.33	0.010331838	48463.9	5	2423.1925	25.03603233
	101317.73	0.010331369	48463.9	15	7269.5775	75.1046871
	101322	0.010331804	46433.8	35	16251.8265	167.9106916
Back face	101317.73	0.010331369	46433.8	35	16251.8265	167.9036153
	101308.53	0.010330431	46433.8	20	9286.758	95.93621091
	101303.93	0.010329962	46433.8	7	3250.3653	33.5761492
	101299.33	0.010329493	46433.8	3	1393.0137	14.38912482

During the calculation when converted pressure from Pa into Kg/mm^2 as our area by mm^2, the created forces were by Kg but when we move to calculate the F we convert force to Newton to calculate produced moment by N.m.
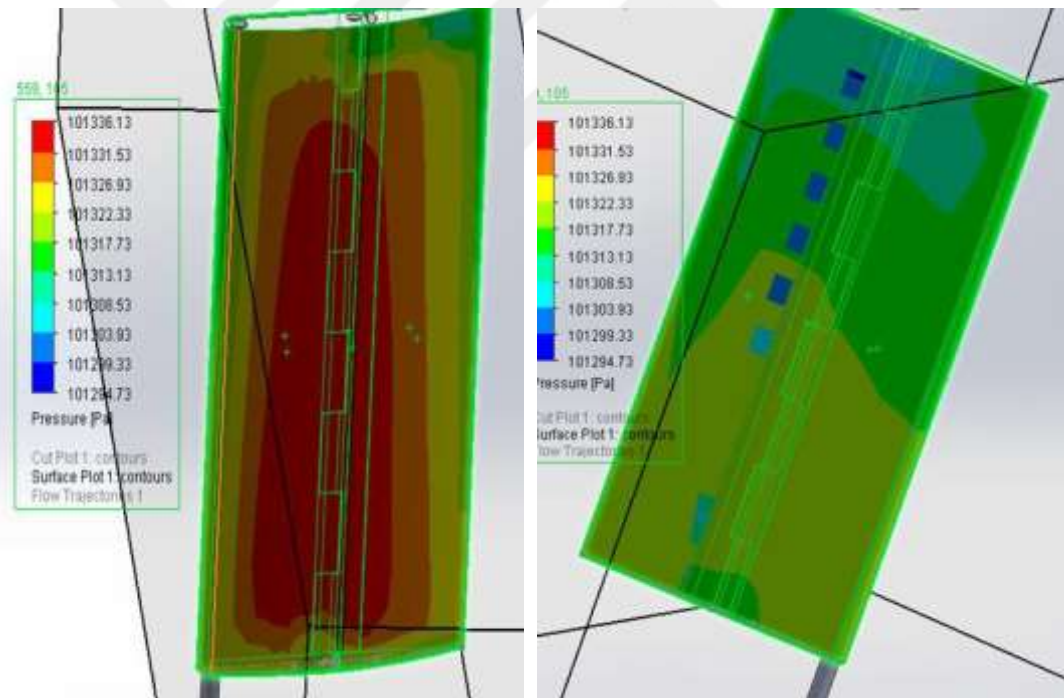
a. Pressure on the front face of the blade

b. Pressure on the back face of the blade

Figure 4.3 Pressure distribution on blade faces where β equal to 10°.

Table 4.3 The produced forces when α = 7°, β = 13° & γ=77°.

Blade Faces	Pressure / Pa	Pressure Kg/mm^2	Area mm^2	Area %	Area subjected to pressure /mm^2	Force / Kg
Front face	101357.03	0.010335376	48463.9	25	12115.9625	125.223
	101349.64	0.010334623	48463.9	30	14539.155	150.2567
	101342.24	0.010333868	48463.9	25	12115.9625	125.2048
	101334.85	0.010333115	48463.9	15	7269.5775	75.11738
	101327.46	0.010332361	48463.9	5	2423.1925	25.0373
	101349.64	0.010334623	46433.8	3	1393.0137	14.39627
Back face	101334.85	0.010333115	46433.8	2	928.6758	9.596114
	101327.46	0.010332361	46433.8	60	27860.274	287.8624
	101320.06	0.010331607	46433.8	30	13930.137	143.9207
	101305.27	0.010330098	46433.8	5	2321.6895	23.98328

a. Pressure on the front face of the blade   b. Pressure on the back face of the blade

Figure 4.4 Pressure distribution on blade faces where β equal to 13°.

Table 4.4 The produced forces when α = 7°, β = 15° & γ=75°

Blade Faces	Pressure / Pa	Pressure Kg/mm^2	Area mm^2	Area %	Area subjected to pressure /mm^2	Force / Kg
Front face	101357.03	0.010335376	48463.9	25	12115.9625	125.223
	101349.64	0.010334623	48463.9	30	14539.155	150.2567
	101342.24	0.010333868	48463.9	25	12115.9625	125.2048
	101334.85	0.010333115	48463.9	15	7269.5775	75.11738
	101327.46	0.010332361	48463.9	5	2423.1925	25.0373
	101349.64	0.010334623	46433.8	3	1393.0137	14.39627
Back face	101334.85	0.010333115	46433.8	2	928.6758	9.596114
	101327.46	0.010332361	46433.8	60	27860.274	287.8624
	101320.06	0.010331607	46433.8	30	13930.137	143.9207
	101305.27	0.010330098	46433.8	5	2321.6895	23.98328

a. Pressure on the front face of the blade   b. Pressure on the back face of the blade

Figure 4.5 Pressure distribution on blade faces where β equal to 15°.

Table 4.5 The produced forces when α = 7°, β = 16° & γ=74°

Blade Faces	Pressure / Pa	Pressure Kg/mm^2	Area mm^2	Area %	Area subjected to pressure /mm^2	Force / Kg
Front face	101349.64	21808.7325	48463.9	45	21808.7325	225.385
	101342.24	7269.5775	48463.9	15	7269.5775	75.12286
	101334.85	9692.77	48463.9	20	9692.77	100.1565
	101327.46	4846.385	48463.9	10	4846.385	50.0746
	101320.06	4846.385	48463.9	10	4846.385	50.07094
	101320.06	11608.4475	46433.8	25	11608.4475	119.9339
Back face	101305.27	9286.758	46433.8	20	9286.758	95.93312
	101297.88	24145.5708	46433.8	52	24145.5708	249.4079
	0	0	46433.8	0	0	0

a. Pressure on the front face of the blade   b. Pressure on the back face of the blade

Figure 4.6 Pressure distribution on blade faces where β equal to 16°.

Table 4.6 The produced forces when α = 7°, β = 17° & γ=73°.

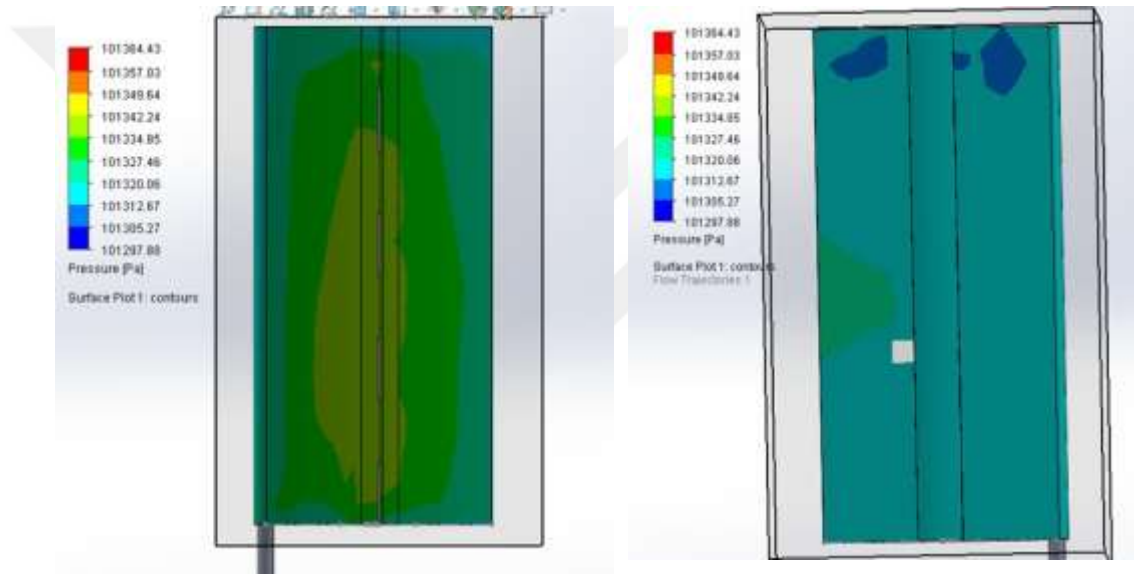| Blade Faces	Pressure / Pa	Pressure Kg/mm^2	Area mm^2	Area %	Area subjected to pressure /mm^2	Force / Kg
Front face	101349.64	0.010334623	48463.9	33	15993.0705	165.2824
	101334.85	0.010333115	48463.9	40	19385.54	200.313
	101327.46	0.010332361	48463.9	20	9692.77	100.1492
	101320.06	0.010331607	48463.9	8	3877.108	40.05675
	0	0	0	0	0	0
Back face	101349.64	0.010334623	46433.8	84	39004.3836	403.0956
	101334.85	0.010333115	46433.8	7	3250.3653	33.5864
	101327.46	0.010332361	46433.8	8	3714.7032	38.38165

a. Pressure on the front face of the blade   b. Pressure on the back face of the blade

Figure 4.7 Pressure distribution on blade faces where β equal to 17°.

Table 4.7 The produced forces when α = 7°, β = 20° & γ=70°

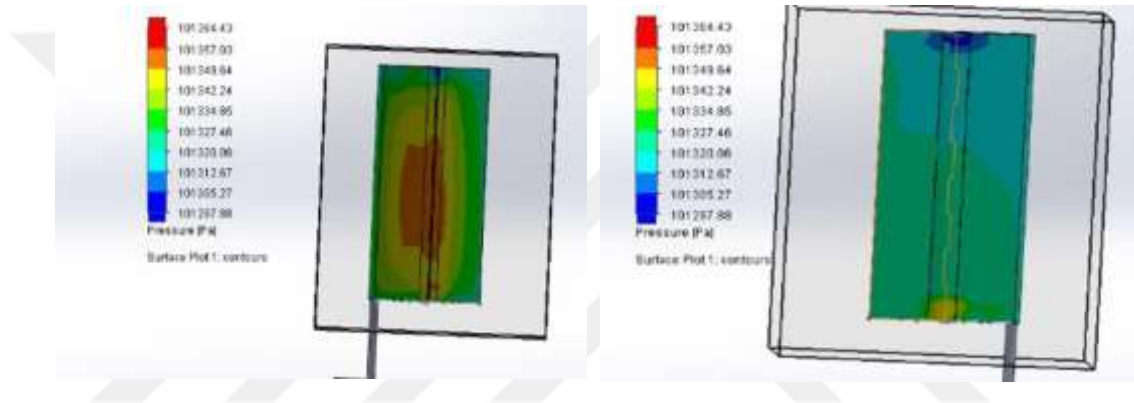| Blade Faces	Pressure / Pa	Pressure Kg/mm^2	Area mm^2	Area %	Area subjected to pressure /mm^2	Force / Kg
Front face	101369.36	0.010336634	48463.9	80	38771.08	400.7624
	101326.06	0.010332218	48463.9	20	9692.77	100.1478
	0	0	48463.9	0	0	0
	0	0	48463.9	0	0	0
	0	0	0	0	0	0
Back face	101369.36	0.010336634	46433.8	2	928.6758	9.599382
	101326.06	0.010332218	46433.8	95	44112.1005	455.7759
	101239.46	0.010323388	46433.8	3	1393.0137	14.38062
	0	0	46433.8	0	0	0

a. Pressure on the front face of the blade   b. Pressure on the back face of the blade

Figure 4.8 Pressure distribution on blade faces where β equal to 20°.

Table 4.8 The produced forces when α = 7°, β = 25° & γ=65°

Blade Faces	Pressure / Pa	Pressure Kg/mm^2	Area mm^2	Area %	Area subjected to pressure /mm^2	Force / Kg
Front face	101369.36	0.010336634	48463.9	74	35863.249	370.7053
	101326.06	0.010332218	48463.9	25	12115.9625	125.1848
	0	0	48463.9	0	0	0
Back face	101369.36	0.010336634	46433.8	100	46433.79	479.9691
	0	0	46433.8	0	0	0

a. Pressure on the front face of the blade   b. Pressure on the back face of the blade

Figure 4.9 Pressure distribution on blade faces where β equal to 25°.

Table 4.9 The produced forces when α = 7°, β = 30° & γ=60°.

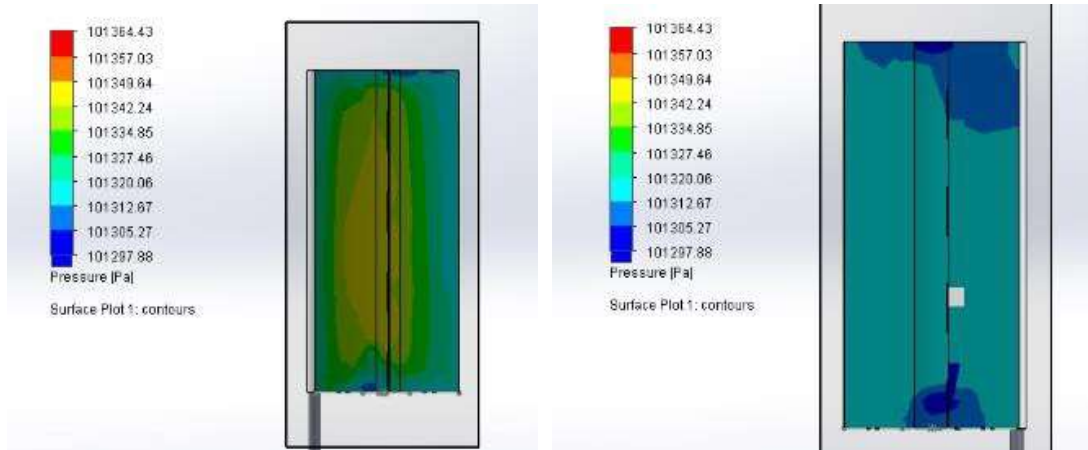| Blade Faces	Pressure / Pa	Pressure Kg/mm^2	Area mm^2	Area %	Area subjected to pressure /mm^2	Force / Kg
Front face	101369.36	0.010336634	48463.9	55	26655.1175	275.5242
	101326.06	0.010332218	48463.9	45	21808.7325	225.3326
	0	0	48463.9	0	0	0
Back face	101369.36	0.010336634	46433.8	100	46433.79	479.9691
	0	0	46433.8	0	0	0

a. Pressure on the front face of the blade   b. Pressure on the back face of the blade

Figure 4.10 Pressure distribution on blade faces where β equal to 30°.

Table 4.10 The produced forces when α = 7°, β = 35° & γ=55°

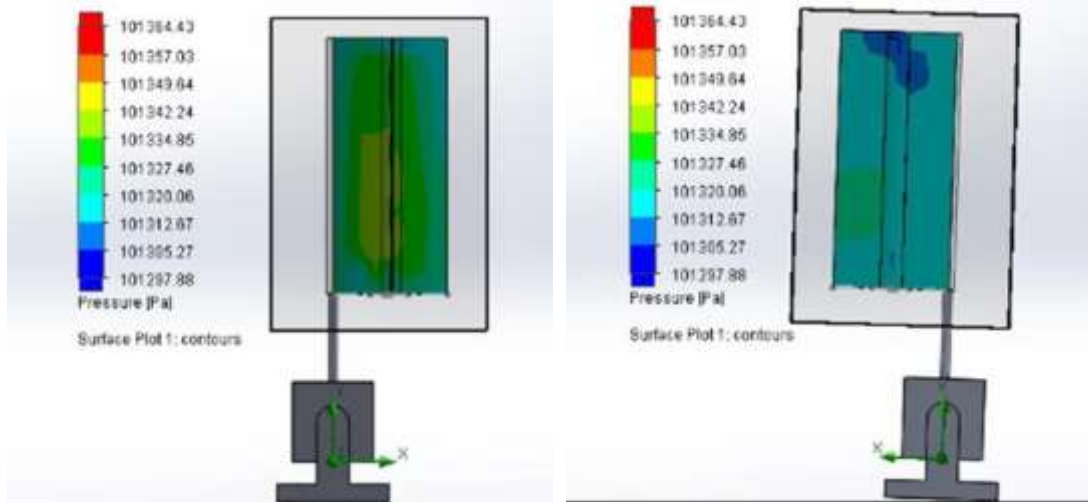| Blade Faces	Pressure / Pa	Pressure Kg/mm^2	Area mm^2	Area %	Area subjected to pressure /mm^2	Force / Kg
Front face	101369.36	0.010336634	48463.9	59	28593.6715	295.5623
	101326.06	0.010332218	48463.9	39	18900.9015	195.2882
	0	0	48463.9	0	0	0
Back face	101369.36	0.010336634	46433.8	100	46433.79	479.9691
	0	0	46433.8	0	0	0

a. Pressure on the front face of the blade   b. Pressure on the back face of the blade

Figure 4.11 Pressure distribution on blade faces where β equal to 35°.

Table 4.11 The produced forces when α = 7°, β = 45° & γ=45°.

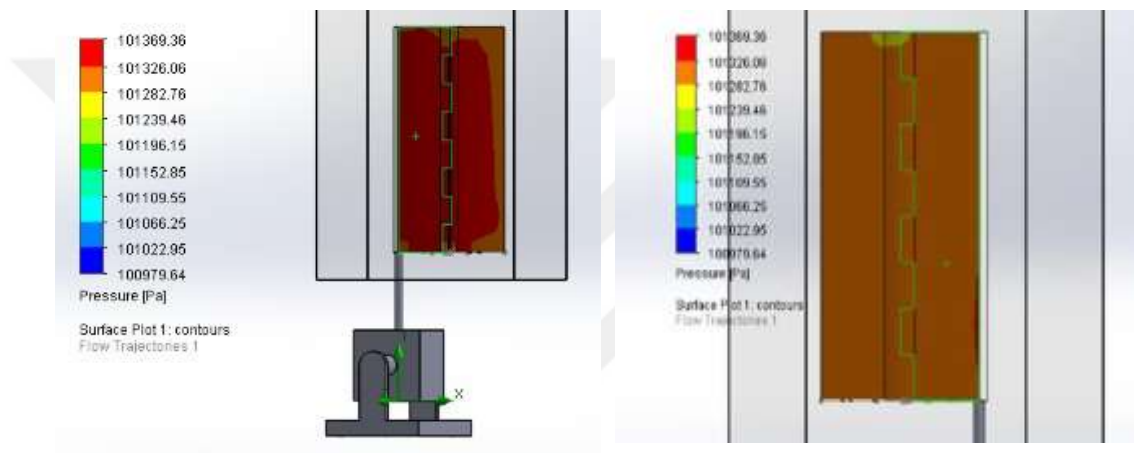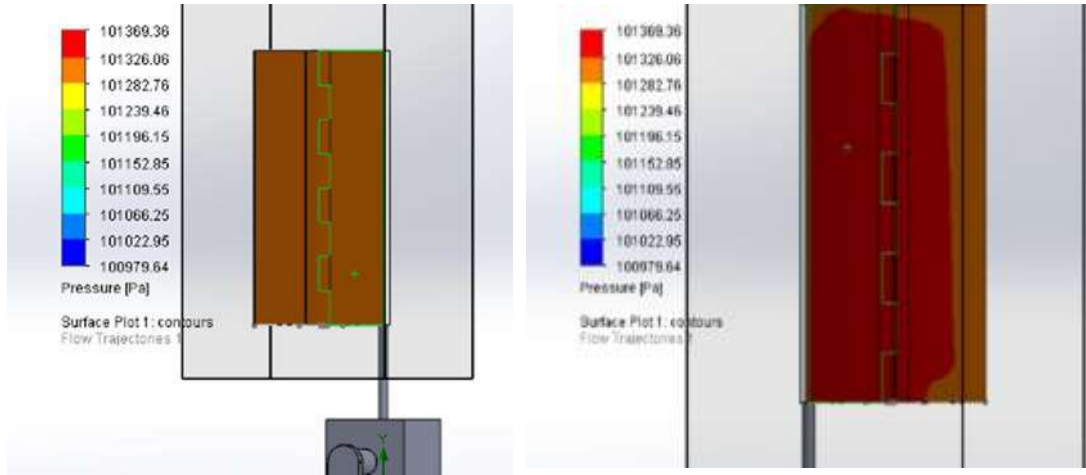| Blade Faces	Pressure / Pa	Pressure Kg/mm^2	Area mm^2	Area %	Area subjected to pressure /mm^2	Force / Kg
Front face	101369.36	0.010336634	48463.9	49	23747.2865	245.467
	101326.06	0.010332218	48463.9	48	23262.648	240.3548
	0	0	48463.9	0	0	0
Back face	101369.36	0.010336634	46433.8	15	6965.0685	71.99536
	101326.06	0.010332218	46433.8	85	39468.7215	407.7994
	0	0	46433.8	0	0	0
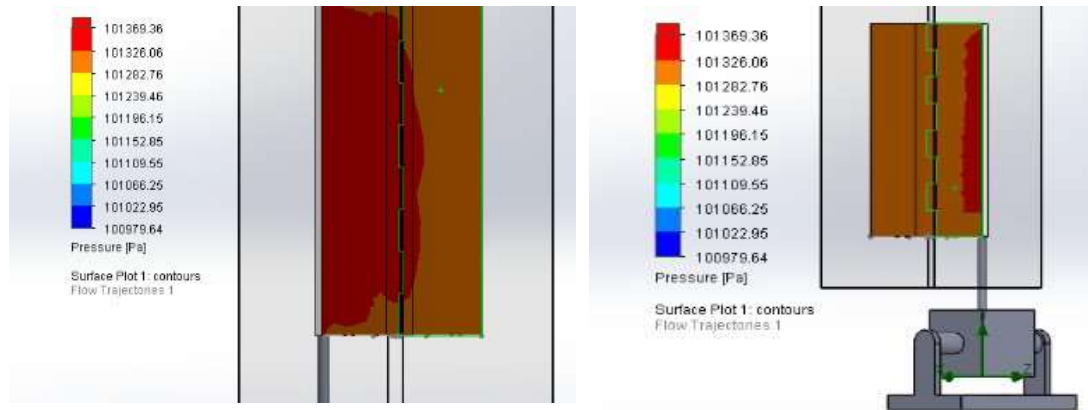
a. Pressure on the front face of the blade   b. Pressure on the back face of the blade

Figure 4.12 Pressure distribution on blade faces where β equal to 45°.

NOTE: when β take the values of 30°, 35° and 45° we ignore 2% of blade area which subjected to pressure that's due to infinitive influence at the tail of the blade.

Table 4.12 The produced moment according to the angle of attack.

β	α	Moment
10°	7°	11.5
13°	7°	31.92
15°	**7°**	**36.7**
16°	7°	30.8
17°	7°	28.3
20°	7°	22.8
25°	7°	21.1
30°	7°	22.1
35°	7°	19.6
45°	7°	13.4

From table 4.12 we can see that when β = 15° the moment (N.M) which rotating the blade is maximum produced torque, now we decide the optimum angle of attack of this blade when the angle between the both parts of the blade is 7° wind velocity is 5 m/sec.

4.3.1.2 Fixed angle of attack

Now, we will move to the second step of our test which considering the best angle of attack equal to 15°. Then, we will start changing the angle between the both parts of the blade to take different values as the following: α = (7°,11°,15°,17.5°,20°), this step aims to determine the best angle between both blade parts when wind velocity is 5

m/s. Calculation were done similar to calculation of section 4.3.1.1, when α = 7° and
β = 15° already studied in the section 4.3.1.1 and produced moment calculated.

Table 4.13 The produced forces when β = 15°, α = 11° & γ 72.8°.

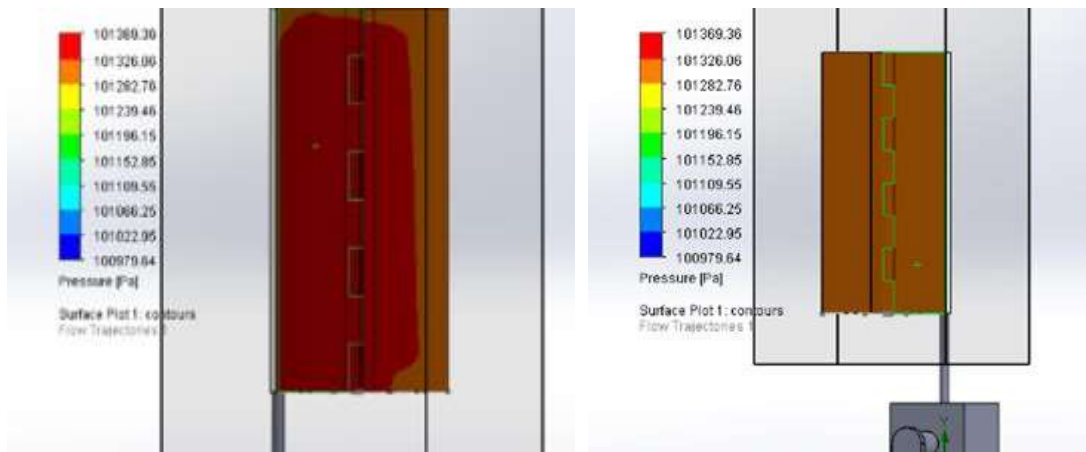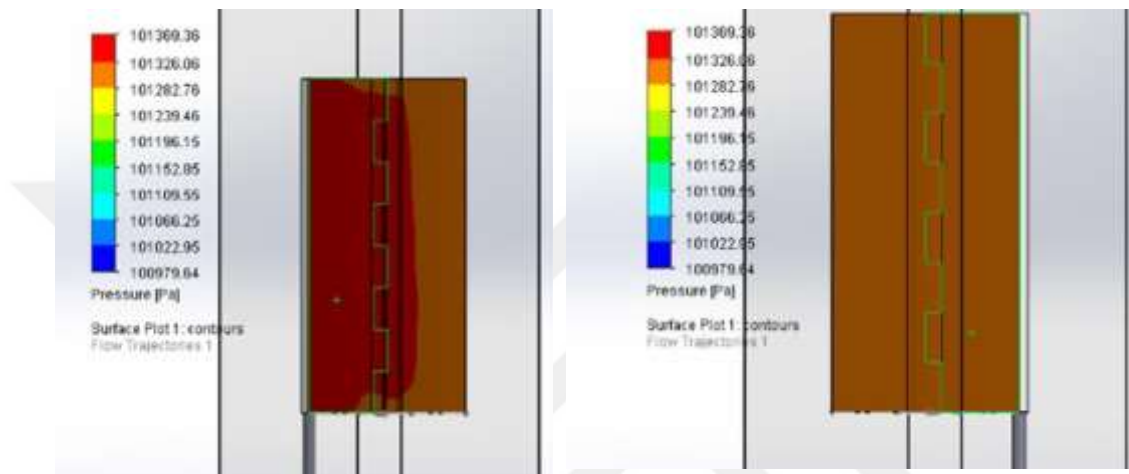| Blade Faces	Pressure / Pa	Pressure Kg/mm^2	Area mm^2	Area %	Area subjected to pressure /mm^2	Force / Kg
Front face	101364.43	0.010336131	48463.9	1	484.6385	5.009287
	101357.03	0.010335376	48463.9	10	4846.385	50.08921
	101349.64	0.010334623	48463.9	39	18900.9015	195.3337
	101342.24	0.010333868	48463.9	19	9208.1315	95.15562
	101334.85	0.010333115	48463.9	19	9208.1315	95.14868
	101327.46	0.010332361	48463.9	10	4846.385	50.0746
	101320.06	0.010331607	48463.9	2	969.277	10.01419
Back face	101342.24	0.010333868	46433.8	7	3250.3653	33.58885
	101334.85	0.010333115	46433.8	10	4643.379	47.98057
	101327.46	0.010332361	46433.8	50	23216.895	239.8853
	101320.67	0.010331669	46433.8	30	13930.137	143.9216
	101312.67	0.010330853	46433.8	2	928.6758	9.594013
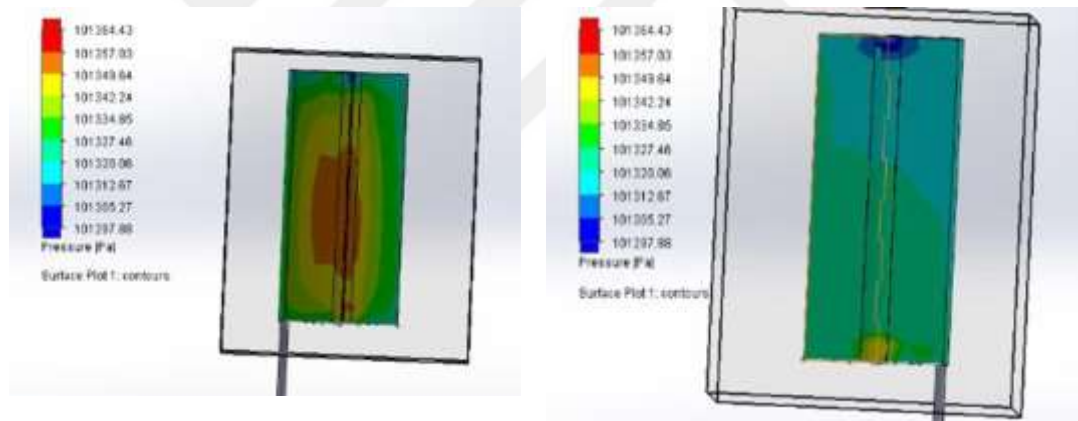
a. Pressure on the front face of the blade   b. Pressure on the back face of the blade

Figure 4.13 Pressure distribution on blade faces where α equal to 11°.

Table 4.14 The produced forces when β = 15°, α = 15° & γ =72.4°.

Blade Faces	Pressure / Pa	Pressure Kg/mm²	Area mm²	Area %	Area subjected to pressure /mm²	Force / Kg
Front face	101364.43	0.010336131	48463.9	25	12115.9625	125.2322
	101357.03	0.010335376	48463.9	20	9692.77	100.1784
	101349.64	0.010334623	48463.9	20	9692.77	100.1711
	101342.24	0.010333868	48463.9	15	7269.5775	75.12286
	101334.85	0.010333115	48463.9	10	4846.385	50.07825
Back face	101327.46	0.010332361	48463.9	10	4846.385	50.0746
	101320.06	0.010331607	48463.9	5	2423.1925	25.03547
	101327.46	0.010332361	46433.8	40	18573.516	191.9083
	101320.06	0.010331607	46433.8	58	26931.5982	278.2467
	101312.67	0.010330853	46433.8	2	928.6758	9.594013

a. Pressure on the front face of the blade   b. Pressure on the back face of the blade

Figure 4.14 Pressure distribution on blade faces where α equal to 15°.

Table 4.15 The produced forces when β = 15°, α = 17.5° & γ =73.1°.

Blade Faces	Pressure / Pa	Pressure Kg/mm^2	Area mm^2	Area %	Area subjected to pressure /mm^2	Force / Kg
Front face	101349.64	0.010334623	48463.9	35	16962.3475	175.2995
	101342.24	0.010333868	48463.9	20	9692.77	100.1638
	101334.85	0.010333115	48463.9	20	9692.77	100.1565
	101327.46	0.010332361	48463.9	20	9692.77	100.1492
	101320.06	0.010331607	48463.9	5	2423.1925	25.03547
	0	0	48463.9	0	0	0
Back face	101342.24	0.010333868	46433.8	2	928.6758	9.596813
	101334.85	0.010333115	46433.8	10	4643.379	47.98057
	101327.46	0.010332361	46433.8	43	19966.5297	206.3014
	101320.06	0.010331607	46433.8	43	19966.5297	206.2863
	101312.67	0.010330853	46433.8	2	928.6758	9.594013

a. Pressure on the front face of the blade

b. Pressure on the back face of the blade

Figure 4.15 Distribution on blade faces where α equal to 17.5°.

Table 4.16 The produced forces when β = 15°, α = 20° & γ =73°.

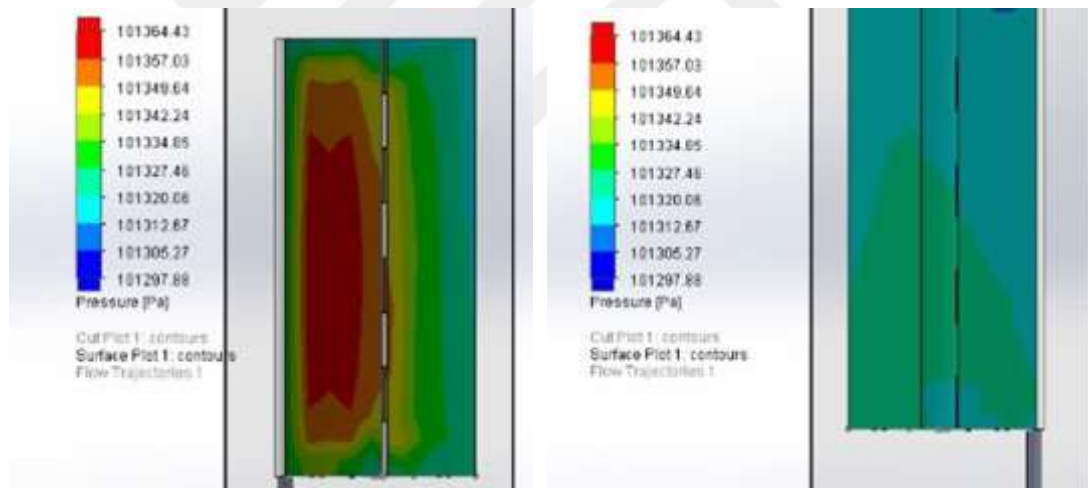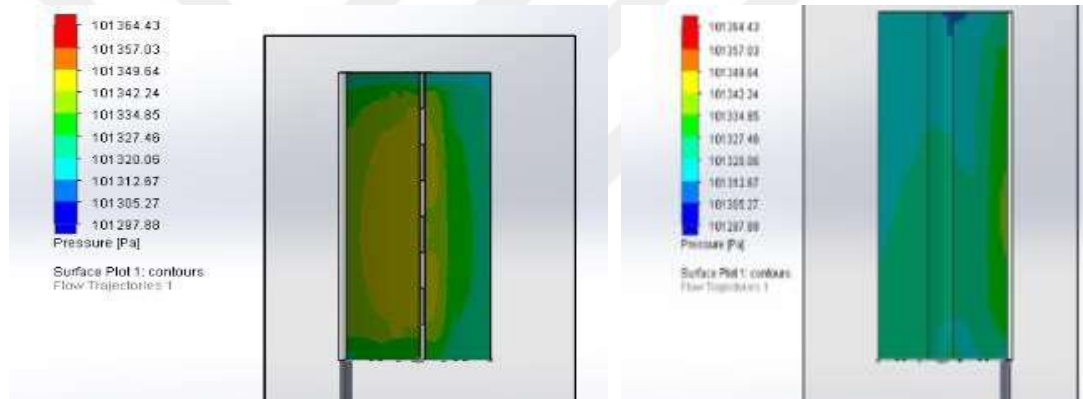| Blade Faces	Pressure / Pa	Pressure Kg/mm^2	Area mm^2	Area %	Area subjected to pressure /mm^2	Force / Kg
Front face	101364.43	0.010336131	48463.9	30	14539.155	150.2786
	101357.03	0.010335376	48463.9	20	9692.77	100.1784
	101349.64	0.010334623	48463.9	10	4846.385	50.08556
	101342.24	0.010333868	48463.9	10	4846.385	50.0819
	101334.85	0.010333115	48463.9	10	4846.385	50.07825
	101327.46	0.010332361	48463.9	10	4846.385	50.0746
	101320.06	0.010331607	48463.9	10	4846.385	50.07094
Back face	101327.46	0.010332361	46433.8	35	16251.8265	167.9197
	101320.06	0.010331607	46433.8	60	27860.274	287.8414
	101312.67	0.010330853	46433.8	4	1857.3516	19.18803
	101305.27	0.010330098	46433.8	1	464.3379	4.796656
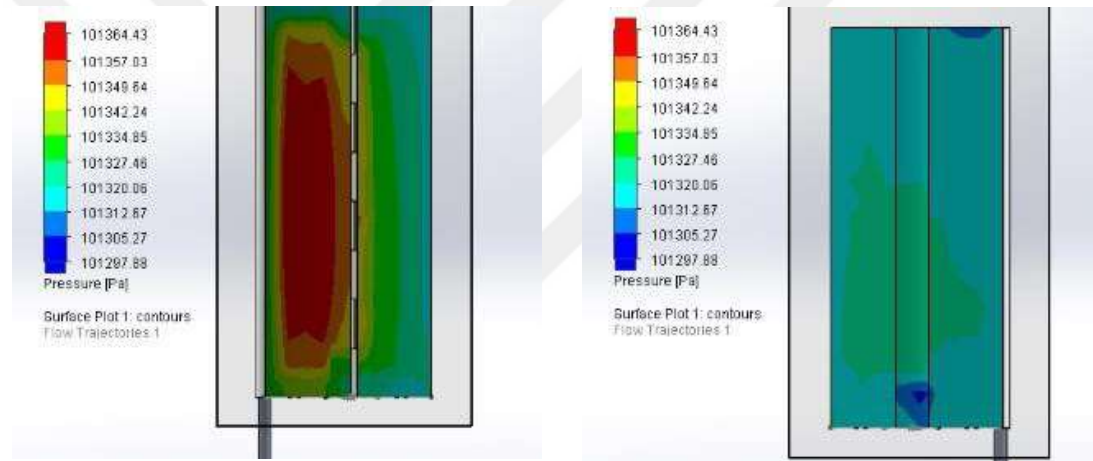
a. Pressure on the front face of the blade   b. Pressure on the back face of the blade

Figure 4.16 Pressure distribution on blade faces where α equal to 20°.

Table 4.17 Moment and different angles between both blade parts.

α	β	Moment
7°	15°	36.7
11°	15°	20.6
15°	15°	46
17.5°	15°	20.08
20°	15°	20.3

From table 4.17 we can see that the moment reached best values when the angle between the two parts α=15° and the angle of attack is 15° as well. When wind velocity changes the results change, we repeat the study with wind velocity of 8 m/sec. The angle between both blade parts is fix α = 7° and we change the angle of attack

according to the following values:

β = (10°,13°,16°,17°,20°,24°,25°,26°,27°,30°,35°) to determine the best angle of attack for this blade model when wind velocity became 8 m/sec.

Table 4.18 The produced forces when α = 7°, β = 10° & γ =80°.

| Blade Faces	Pressure / Pa	Pressure Kg/mm^2	Area mm^2	Area %	Area subjected to pressure /mm^2	Force / Kg
Front face	101408.1	0.010340584	48463.9	75	36347.8875	375.8584
	101343.1	0.010333956	48463.9	25	12115.9625	125.2058
	0	0	48463.9	0	0	0
Back face	101343.1	0.010333956	46433.8	99	45969.4521	475.0463
	101213.09	0.010320699	46433.8	1	464.3379	4.792292
	0	0	46433.8	0	0	0

a. Pressure on the front face of the blade   b. Pressure on the back face of the blade

Figure 4.17 Pressure distribution on blade faces where β equal to 10°.

Table 4.19 The produced forces when α = 7°, β = 13° & γ =77°.

Blade Faces	Pressure / Pa	Pressure Kg/mm^2	Area mm^2	Area %	Area subjected to pressure /mm^2	Force / Kg
Front face	101408.1	0.010340584	48463.9	75	36347.8875	375.8584
	101343.1	0.010333956	48463.9	25	12115.9625	125.2058
	0	0	48463.9	0	0	0
Back face	101343.1	0.010333956	46433.8	99	45969.4521	475.0463
	101213.09	0.010320699	46433.8	1	464.3379	4.792292
	0	0	46433.8	0	0	0

a. Pressure on the front face of the blade   b. Pressure on the back face of the blade

Figure 4.18 Pressure distribution on blade faces where β equal to 13°.

Table 4.20 The produced forces when α = 7°, β = 16° & γ =74°.

Blade Faces	Pressure / Pa	Pressure Kg/mm^2	Area mm^2	Area %	Area subjected to pressure /mm^2	Force / Kg
Front face	101408.1	0.010340584	48463.9	50	24231.925	250.5723
	101343.1	0.010333956	48463.9	50	24231.925	250.4116
	0	0	48463.9	0	0	0
Back face	101343.1	0.010333956	46433.8	99	45969.4521	475.0463
	101213.09	0.010320699	46433.8	1	464.3379	4.792292
	0	0	46433.8	0	0	0

a. Pressure on the front face of the blade   b. Pressure on the back face of the blade

Figure 4.19 Pressure distribution on blade faces where β equal to 16°.

41

Table 4.21 The produced forces when α = 7°, β = 17° & γ =73°.

Blade Faces	Pressure / Pa	Pressure Kg/mm^2	Area mm^2	Area %	Area subjected to pressure /mm^2	Force / Kg
Front face	101408.1	0.010340584	48463.9	45	21808.7325	225.515
	101343.1	0.010333956	48463.9	55	26655.1175	275.4528
	0	0	48463.9	0	0	0
Back face	101343.1	0.010333956	46433.8	100	46433.79	479.8447
	0	0	46433.8	0	0	0

a. Pressure on the front face of the blade   b. Pressure on the back face of the blade
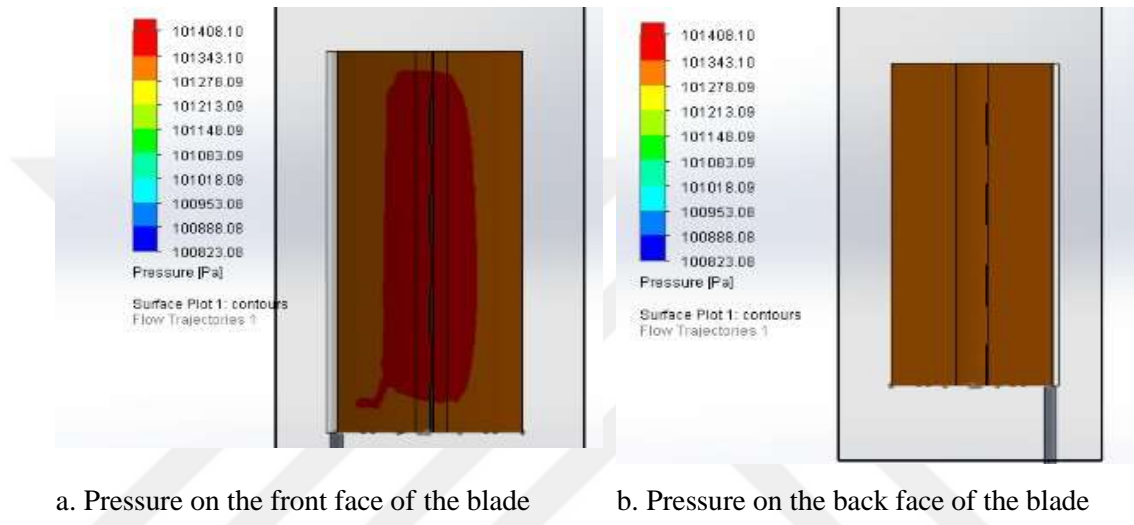
Figure 4.20 Pressure distribution on blade faces where β equal to 17°.

Table 4.22 The produced forces when α = 7°, β = 20° & γ =70°.

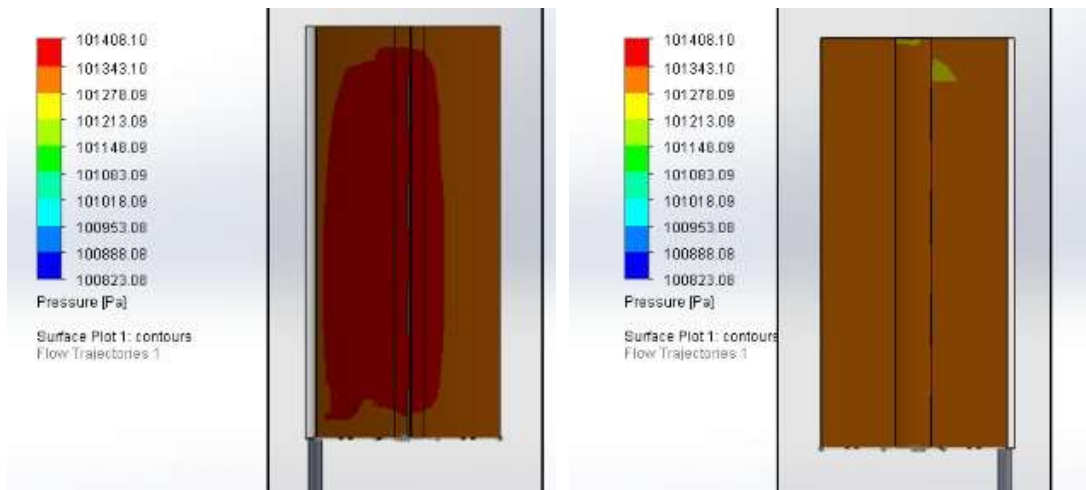| Blade Faces	Pressure / Pa	Pressure Kg/mm^2	Area mm^2	Area %	Area subjected to pressure /mm^2	Force / Kg
Front face	101408.1	0.010340584	48463.9	30	14539.155	150.3434
	101343.1	0.010333956	48463.9	70	33924.695	350.5763
	0	0	48463.9	0	0	0
Back face	101343.1	0.010333956	46433.8	99	45969.4521	475.0463
	101213.09	0.010320699	46433.8	1	464.3379	4.792292
	0	0	46433.8	0	0	0
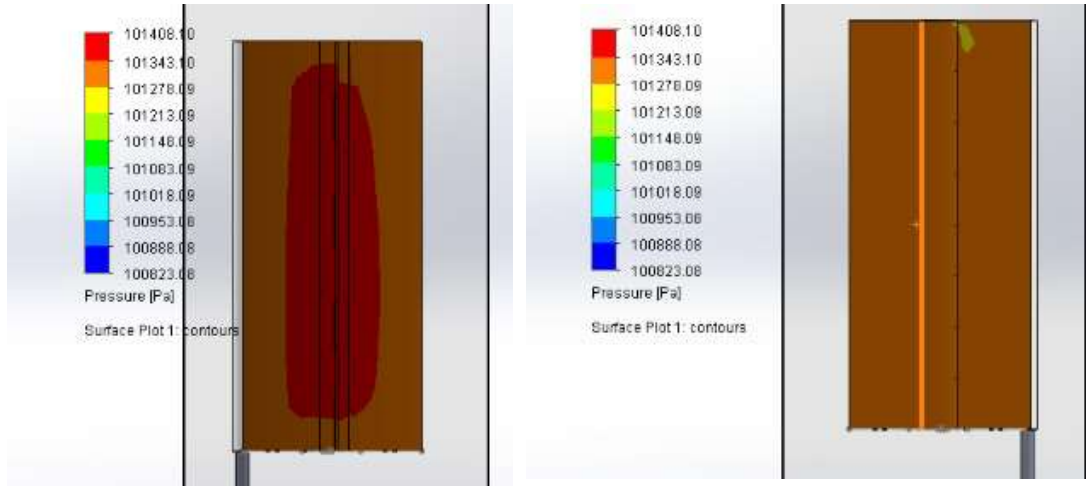
a. Pressure on the front face of the blade   b. Pressure on the back face of the blade

Figure 4.21 Pressure distribution on blade faces where β equal to 20°.

Table 4.23 The produced forces when α = 7°, β = 24° & γ =66°.

Blade Faces	Pressure / Pa	Pressure Kg/mm^2	Area mm^2	Area %	Area subjected to pressure /mm^2	Force / Kg
Front face	101408.1	0.010340584	48463.9	80	38771.08	400.9156
	101343.1	0.010333956	48463.9	20	9692.77	100.1647
	0	0	48463.9	0	0	0
Back face	101343.1	0.010333956	46433.8	100	46433.79	479.8447
	0	0	46433.8	0	0	0

a. Pressure on the front face of the blade   b. Pressure on the back face of the blade

Figure 4.22 Pressure distribution on blade faces where β equal to 24°.

Table 4.24 The produced forces when α = 7°, β = 25° & γ =65°.

Blade Faces	Pressure / Pa	Pressure Kg/mm^2	Area mm^2	Area %	Area subjected to pressure /mm^2	Force / Kg
Front face	101408.1	0.010340584	48463.9	69	33440.0565	345.7897
	101343.1	0.010333956	48463.9	30	14539.155	150.247
	0	0	48463.9	0	0	0
Back face	101343.1	0.010333956	46433.8	100	46433.79	479.8447
	0	0	46433.8	0	0	0

a. Pressure on the front face of the blade   b. Pressure on the back face of the blade

Figure 4.23 Pressure distribution on blade faces where β equal to 25°.

Table 4.25 The produced forces when α = 7°, β = 26° & γ =64°.

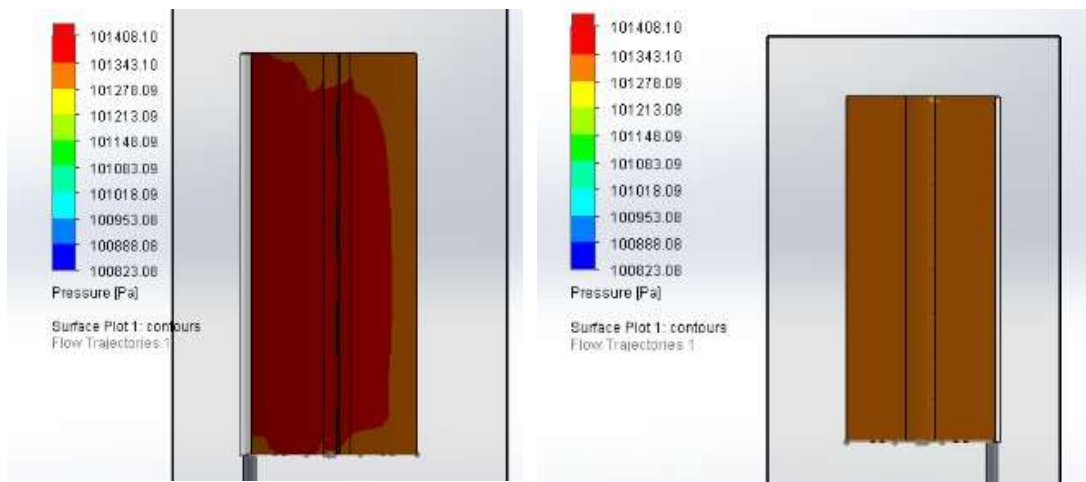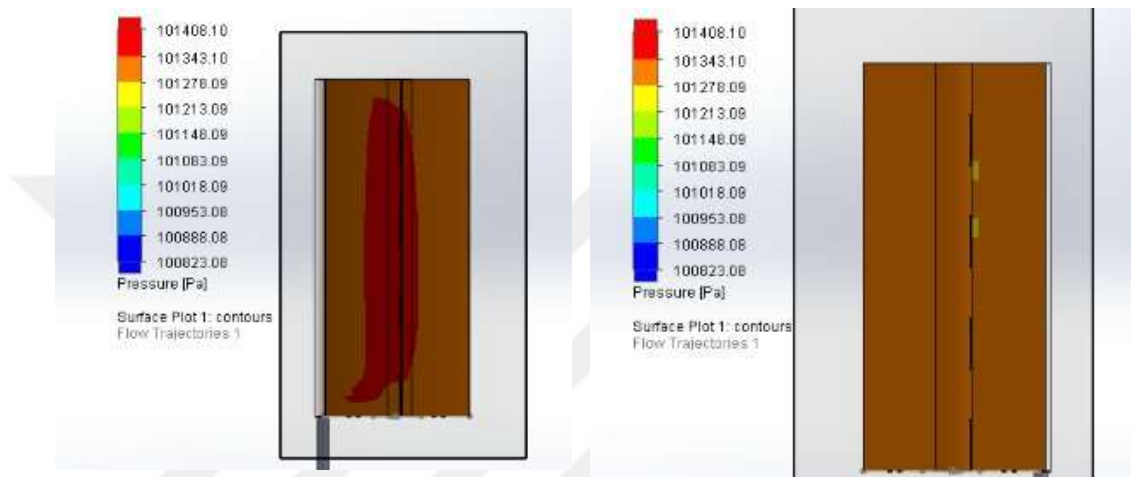| Blade Faces	Pressure / Pa	Pressure Kg/mm^2	Area mm^2	Area %	Area subjected to pressure /mm^2	Force / Kg
Front face	101408.1	0.010340584	48463.9	69	33440.0565	345.7897
	101343.1	0.010333956	48463.9	30	14539.155	150.247
	0	0	48463.9	0	0	0
Back face	101343.1	0.010333956	46433.8	100	46433.79	479.8447
	0	0	46433.8	0	0	0

a. Pressure on the front face of the blade   b. Pressure on the back face of the blade

Figure 4.24 Pressure distribution on blade faces where β equal to 26°.

Table 4.26 The produced forces when α = 7°, β = 27° & γ =63°.

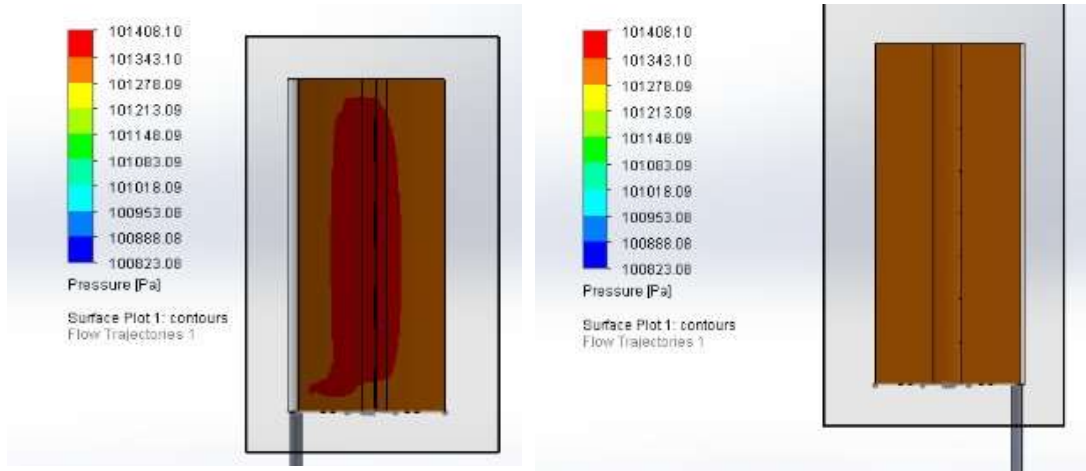| Blade Faces	Pressure / Pa	Pressure Kg/mm^2	Area mm^2	Area %	Area subjected to pressure /mm^2	Force / Kg
Front face	101408.1	0.010340584	48463.9	68.5	33197.73725	343.284
	101343.1	0.010333956	48463.9	30	14539.155	150.247
	0	0	48463.9	0	0	0
Back face	101343.1	0.010333956	46433.8	100	46433.79	479.8447
	0	0	46433.8	0	0	0

a. Pressure on the front face of the blade   b. Pressure on the back face of the blade

Figure 4.25 Pressure distribution on blade faces where β equal to 27°.

45

Table 4.27 The produced forces when α = 7°, β = 30° & γ =60°.

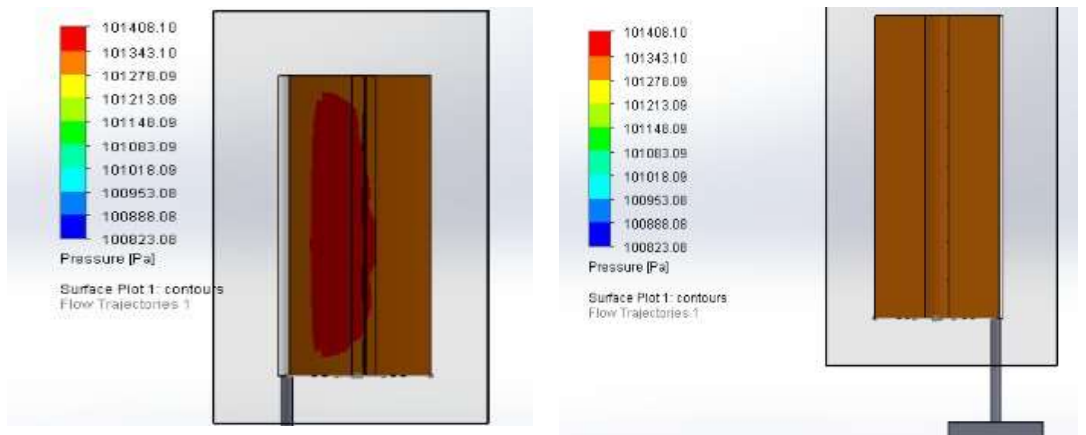| Blade Faces	Pressure / Pa	Pressure Kg/mm2	Area mm2	Area %	Area subjected to pressure / mm2	Force / Kg
Front face	101408.1	0.010340584	48463.9	29	14054.5165	145.3319
	101343.1	0.010333956	48463.9	69	33440.0565	345.5681
	0	0	48463.9	0	0	0
Back face	101343.1	0.010333956	46433.8	100	46433.79	479.8447
	0	0	46433.8	0	0	0

a. Pressure on the front face of the blade   b. Pressure on the back face of the blade

Figure 4.26 Pressure distribution on blade faces where β equal to 30°.

Table 4.28 The produced forces when α = 7°, β = 35° & γ =55°.

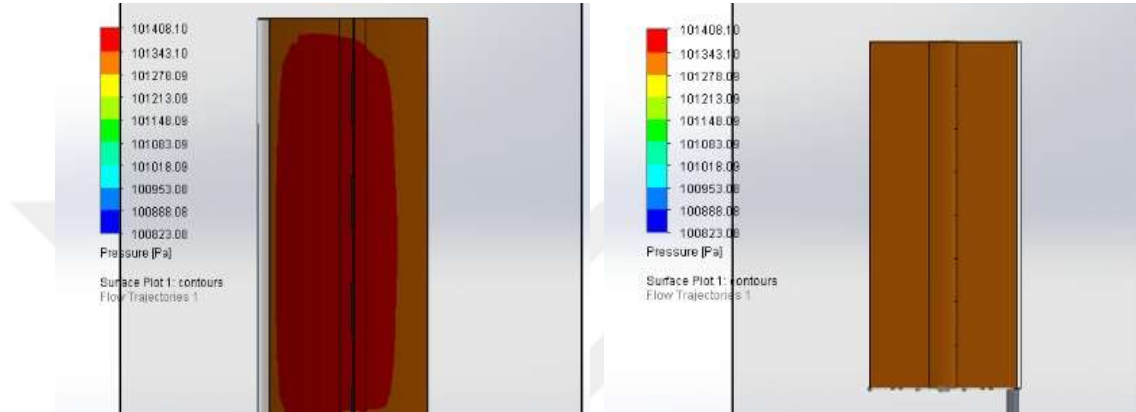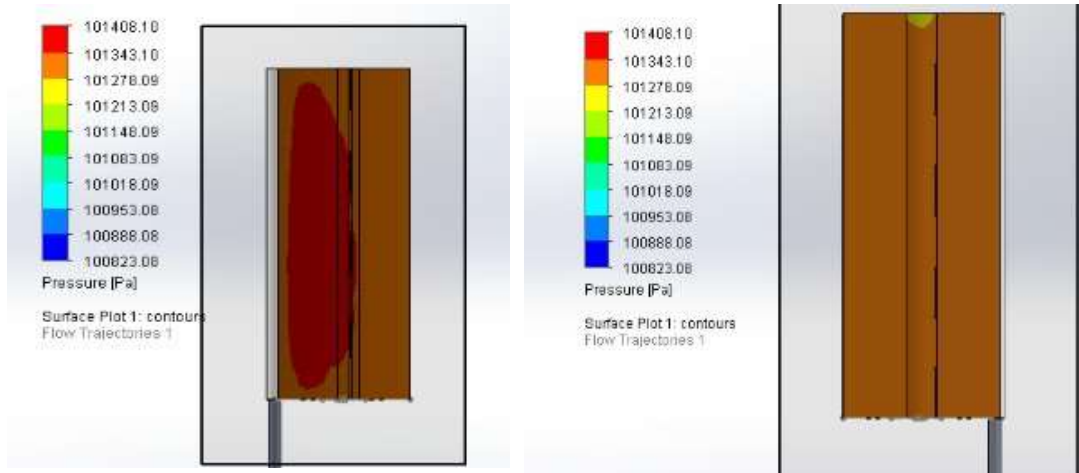| Blade Faces	Pressure / Pa	Pressure Kg/mm2	Area mm2	Area %	Area subjected to pressure / mm2	Force / Kg
Front face	101408.1	0.010340584	48463.9	39	18900.9015	195.4464
	101343.1	0.010333956	48463.9	58	28109.033	290.4775
	0	0	48463.9	0	0	0
Back face	101343.1	0.010333956	46433.8	99	45969.4521	475.0463
	101213.09	0.010320699	46433.8	1	464.3379	4.792292
	0	0	46433.8	0	0	0

a. Pressure on the front face of the blade b. Pressure on the back face of the blade

Figure 4.27 Pressure distribution on blade faces where β equal to 35°.

Table 4.29 Produced moment with different angle of attack.

β	α	Moment
10°	7°	11.8
13°	7°	15.4
16°	7°	22.4
17°	7°	23.06
20°	7°	26.51
24°	**7°**	**34.64**
25°	7°	31.04
26°	7°	28.7
27°	7°	24.26
30°	7°	20.7
35°	7°	13.24

According to table 4.29 we can see that the maximum moment has been achieved when angle of attack is equal to 24°.

4.3.2 Second smart blade model

The second model is a smart blade with a changeable surface able to take different areas according to wind velocity. The blade is consisting of two parts fixed to each other from the root with special joints, figure 4-29 shows the second model.

α is the angle between the both parts of the blade. This angle will take different values in another world we are going to change this angle until we achieved the best outcome moment, as the following α = (0°, 3°, 6°), while wind speed is equal to 8 m/s, besides reaching the best angle of attack for this model we will see how the area affecting wind turbine performance.

47

During the experiment, the area of the blade will change three times. However, wind will face different areas in three cases, a new calculation method has been used in this section, while the inputs enabling the Solid works program from calculating the forces on the X-axis, this force is responsible for rotating the blade, however, same equations have been used in section 4.3.1.
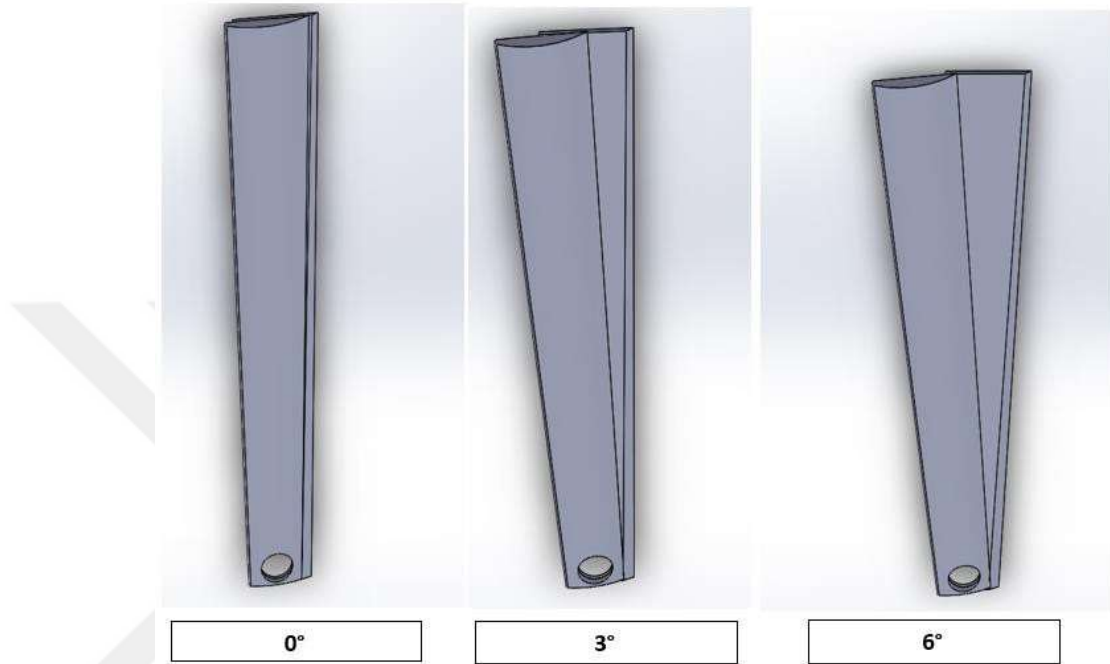
Figure 4.28 Second smart blade model.

4.3.2.1 Angel between both parts equal to 0° the first case:

The first case examined an angle between the two slides of the blade equal to Zero, area subjected to wind attack is 125811.45 mm^2, the rotating arm is b= 472.41*10^{-3} m, the following table explains forces formed on X and Y axises.

Table 4.30 Forces formed on X and Y axises when α=0°

Goal Name	Unit	Value	Averaged Value	Minimum Value	Maximum Value
GG Normal Force 1	[N]	6.76278712	6.740381596	6.72728914	6.76342059
GG Normal Force (X) 1	[N]	-1.06832198	-1.037381215	-1.068686824	-0.97861949
GG Force (X) 1	[N]	-1.06536145	-1.033007795	-1.065361453	-0.974511285
GG Force (Y) 1	[N]	6.69014766	6.672385174	6.659227885	6.690788981

Normal force (X) is F, the force causing blade rotation, using equation (4.3) moment will be calculated, M = 1.068*472.41*10^{-3}→ M = 0.5 N.m.

48

Figure 4.29 Pressure distribution and WF on the FF of the blade from Y-axis when α=0°.

4.3.2.2 Angel between both parts equal to 3° the second case:

The second case examined an angle between the two slides of the blade equal to 3°, area subjected to wind flow is 150554.09 mm², same steps in section 4.3.2.2 has been followed.

Table 4. 31 Forces formed on X and Y axises when α=3°.

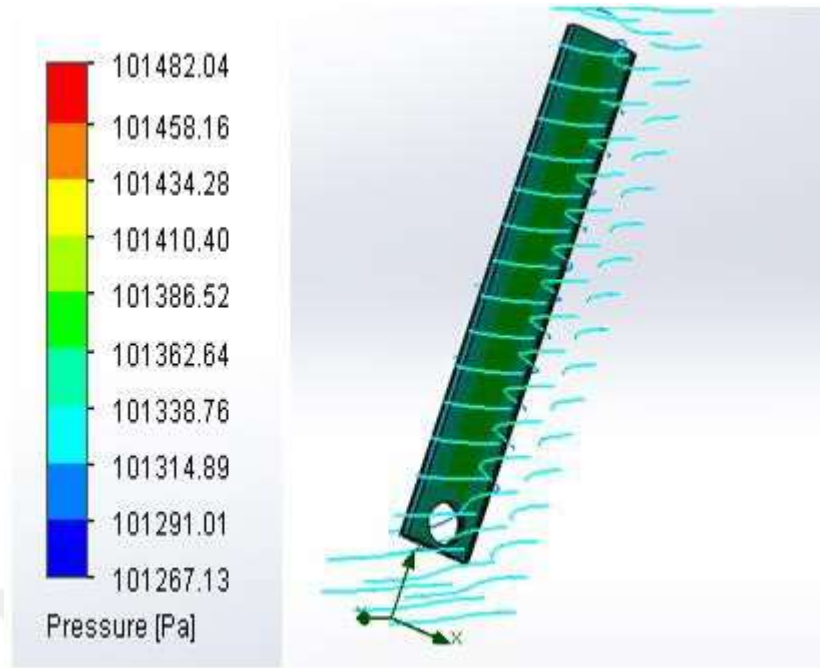| Goal Name	Unit	Value	Averaged Value	Minimum Value	Maximum Value
GG Normal Force 1	[N]	9.73167765	9.658144925	9.568219517	9.992341621
GG Normal Force (X) 1	[N]	-1.37333301	-1.355220781	-1.381295481	-1.332227623
GG Force (X) 1	[N]	-1.37317147	-1.355055271	-1.380342724	-1.331705824
GG Force (Y) 1	[N]	9.64404643	9.572289365	9.484727085	9.906612994

M= 1.37*472.41*10⁻³ → M = 0.64 N.m.

49
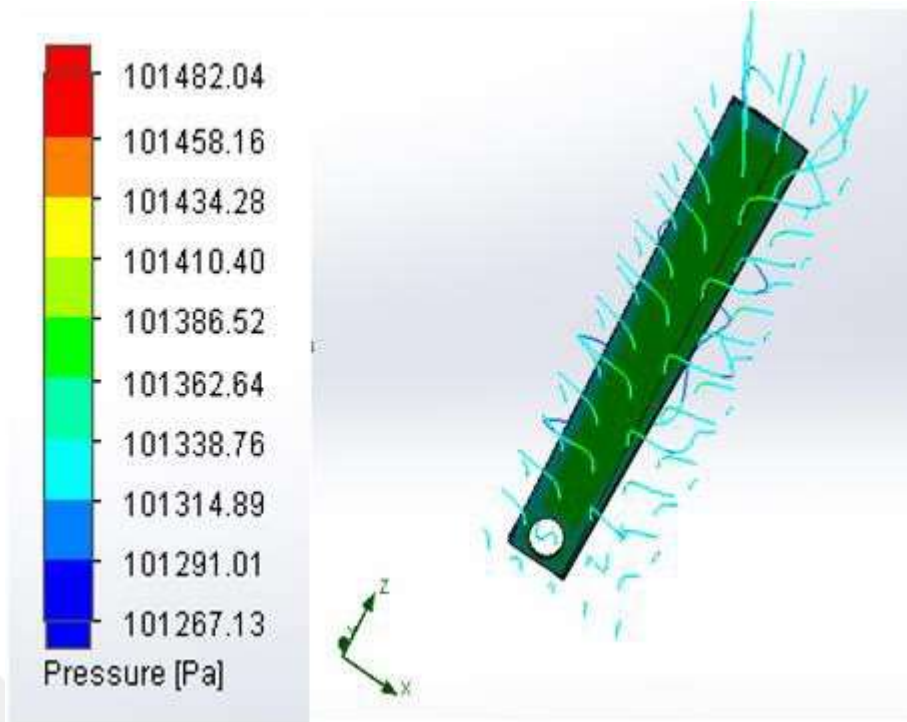
Figure 4.30 Pressure distribution and WF on the FF of the blade from Y-axis when α=3°.

4.3.2.3 Angel between both parts equal to 6° the third case:

The third case examined an angle between the two slides of the blade equal to 6°, area subjected to wind attack is 175282.29 mm², same steps in section 4.3.2.2 has been followed.

Table 4.32 Forces formed on X and Y axises when α=6°.

Goal Name	Unit	Value	Averaged Value	Minimum Value	Maximum Value
GG Normal Force 1	[N]	11.9897873	12.0948466	11.89761326	12.5663019
GG Normal Force (X) 1	[N]	-1.66360071	-1.656347594	-1.741572334	-1.637479103
GG Force (X) 1	[N]	-1.65427211	-1.645544276	-1.731181822	-1.626966062
GG Force (Y) 1	[N]	11.8801593	11.98721329	11.78980987	12.45214811

M= 1.66*472.41*10⁻³ → M = 0.78 N.m.

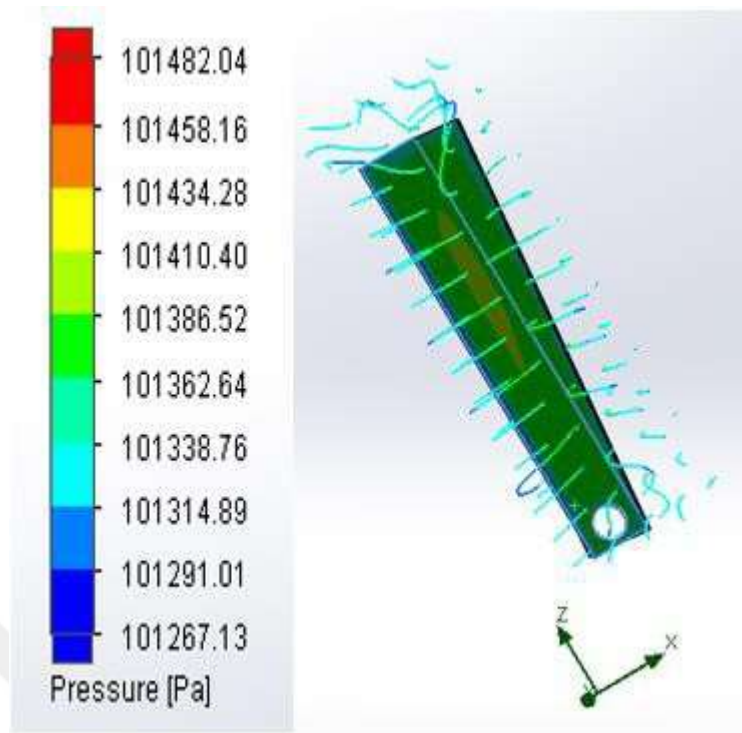**Figure 4.31** Pressure distribution and WF on the FF of the blade from Y-axis when α=6°.

Table 4.33 Produced moment with different angle between both blade faces.

Angle	Area	Moment
0°	125811.45 mm^2	0.5
3°	150554.09 mm^2	0.64
6°	175282.29 mm^2	0.78

51

CHAPTER 5

RESULTS & DISCUSSION

5.1 Introduction

During this chapter, we will summarize the results has been achieved in section 4.1 and 4.2 in the fourth chapter. Wind turbine efficiency can be increased by modeling smart blade which able to variation area together angle (the angle of attack and the angle between the two parts of the blade (α and β) using a specific mechanism and sensors. These sensors can measure wind condition instantly and give an accurate order to address the new angles of the blade.

5.2 First smart blade model

From the first model, we can recognize that we fixed the angle between the two parts of the blade at 7°, which consider the zero point of the model, an airfoil of A NACA 4705 wind turbine blade has been used for the first model. The blade subjected to steady wind velocity 5 m/sec. The wind hits the two blade faces and different pressures formed on the both faces, logically the first face which is the curved face subjected to higher pressure than the back face, the aerodynamic forces have been calculated and we assume that the force which hit the front face is F_a from this force and depending on the complementary angle of the incident angle we calculated F which is the force produce moment or torque which causes blade rotation. Increasing the produced moment meaning increasing the power produced by the wind turbine as simple as it. When $\alpha = 7°$ we change the angle of attack to discover at which value the produced moment is maximum, the following values have been applied and results recorded β = (10°,13°,15°,16°,17°,20°,25°,30°,35°,45°), figures 5. 1,2,3,4,5,6,8,9,10 and 11 are demonstrating the pressure distribution on the front face of the blade when wind come from the Z-axis with different angle of attack.

Figure 5.1 Pressure analysis when wind hits the blade at Z-axis at β=1.

Figure 5.2 Pressure analysis when wind hits the blade at Z-axis at β=13°.

Figure 5.3 Pressure analysis when wind hits the blade at Z-axis at β=20.

Figure 5.4 Pressure analysis when wind hits the blade at Z-axis at β=30°.

Figure 5.5 Pressure analysis when wind hits the blade at Z-axis at β=35°.
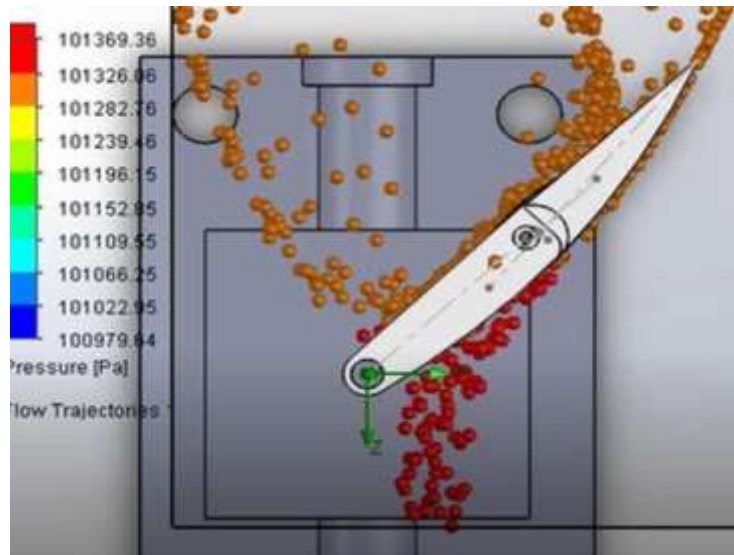
Figure 5.6 Pressure analysis when wind hits the blade at Z-axis at β=45°.

Produced moment has been calculated according to the different angle of attack values as explained in section 4.1 and the following curve appeared.
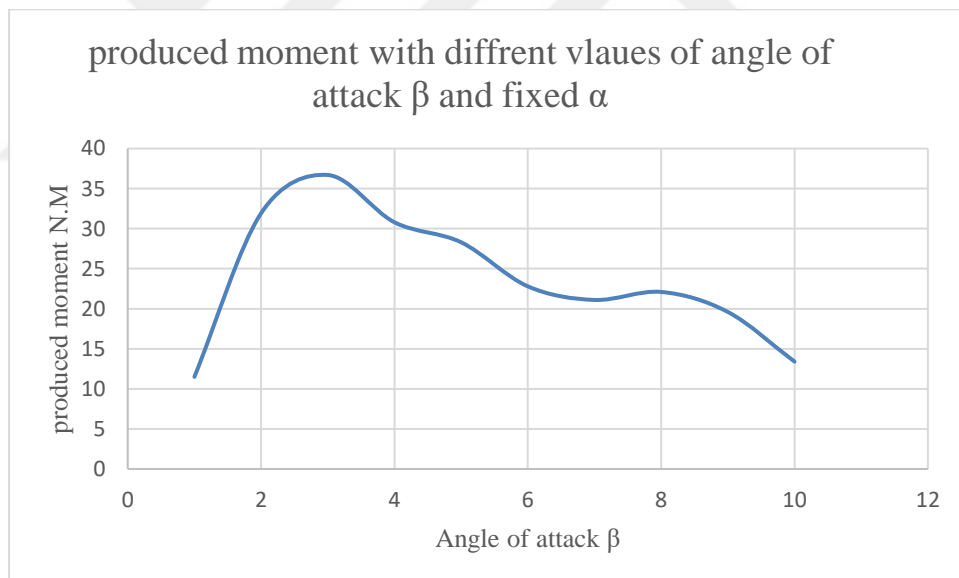
Figure 5.7 Produced moment and the angle of attack with fixed α=7°.

Easley, we can recognize that the best moment has been achieved with the value of angle of attack equal to 15°. Now, we have the optimum angle of attack, hence, we can search for the best angle between the two parts of the blade, as mentioned in chapter four in section 4.1, by this way we can reach the best performance of the wind turbine at the given wind velocity. Back to our concept, we assume β=15°, and α= 7°,11°,15°,17.5°,20°.

Produced moment calculated by the same approach and the results that lead us to the best angle between the two parts of the blade, results are showed in fig 5.13.
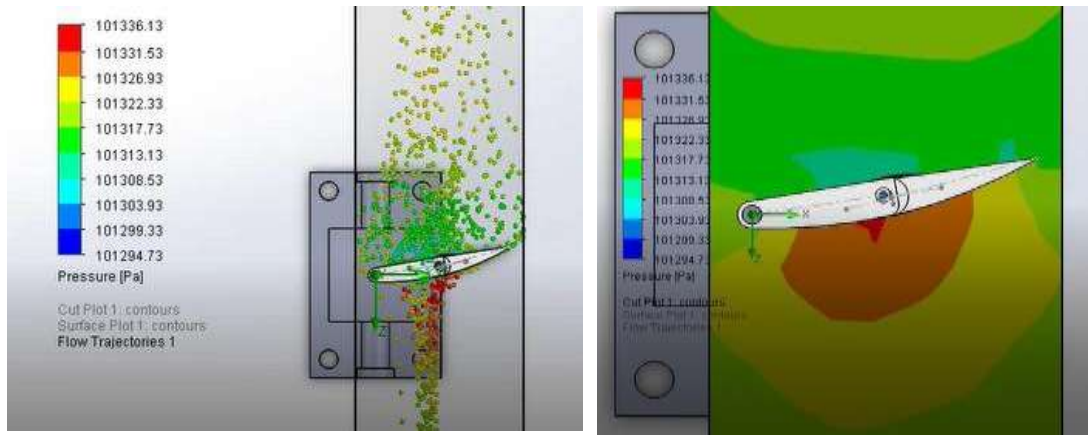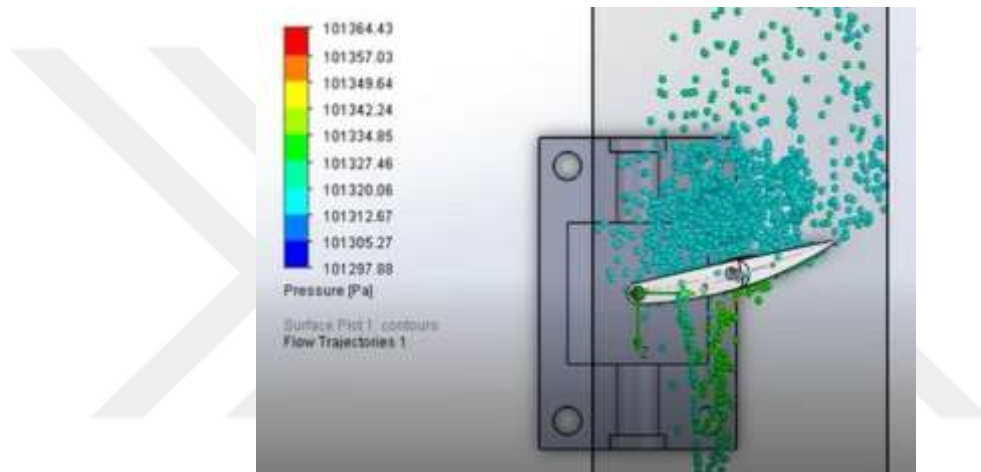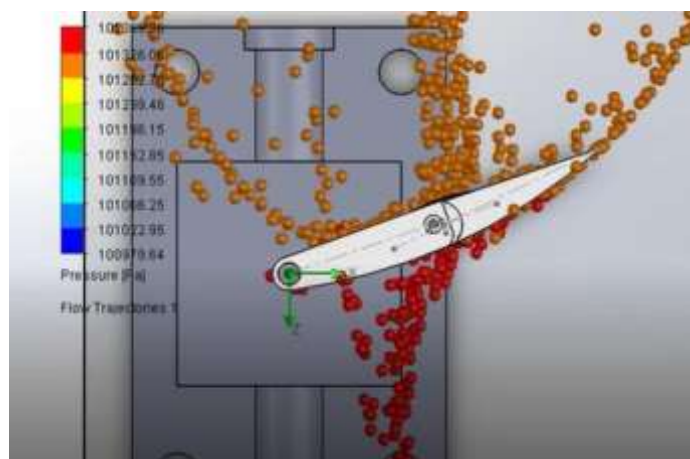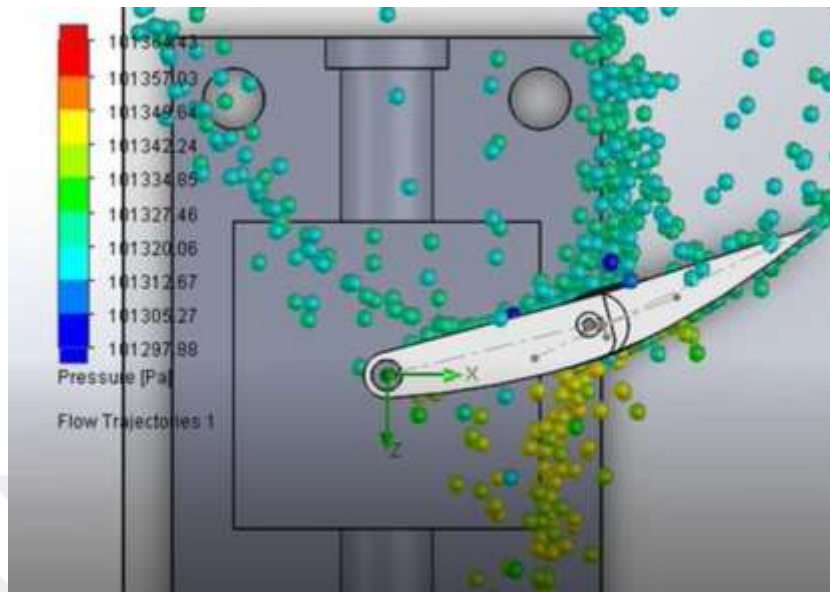

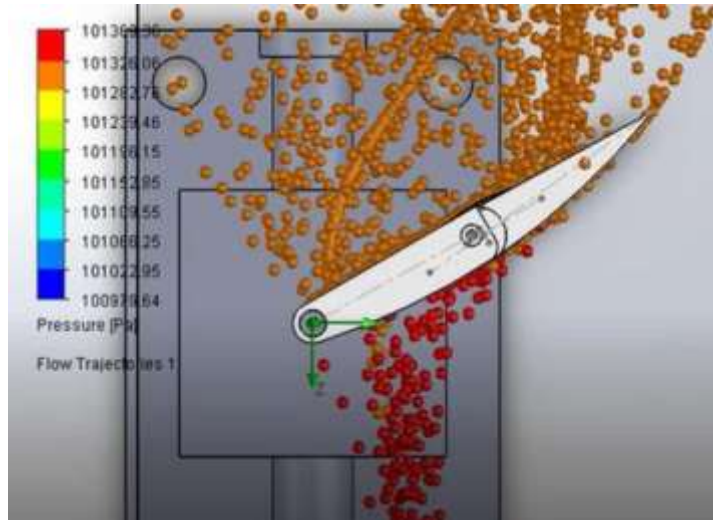**Figure 5.8** Pressure analysis when wind hits the blade at Z-axis at α=11°.

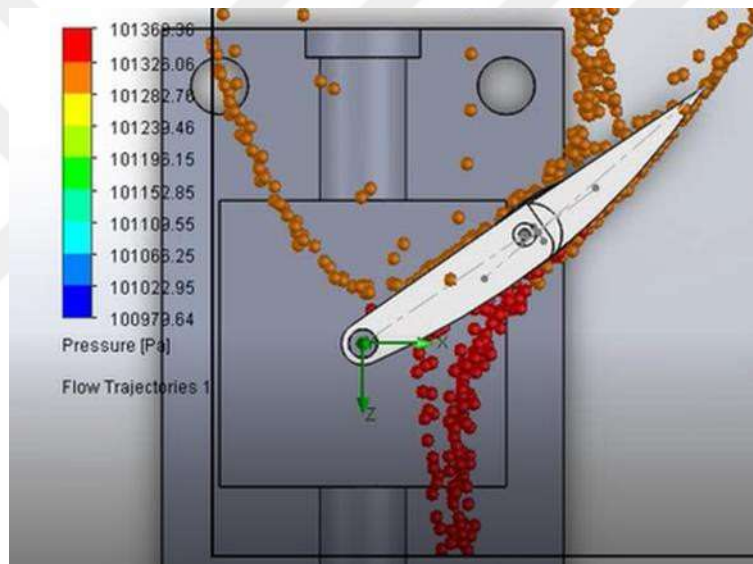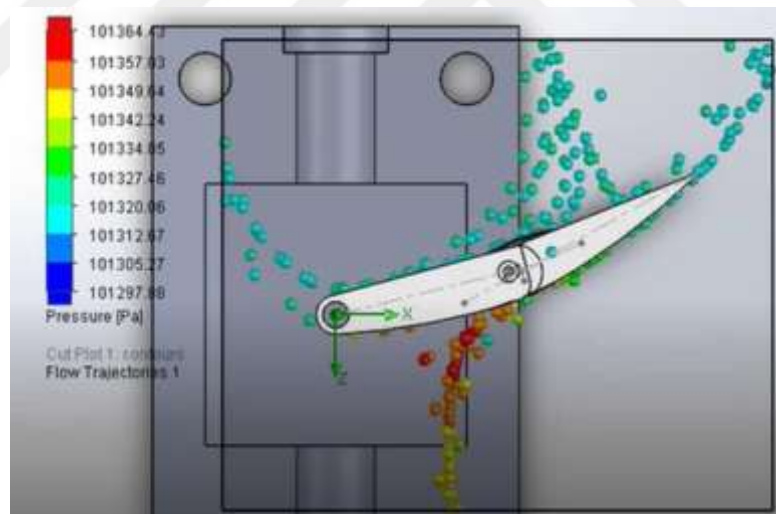**Figure 5.9** Pressure analysis when wind hits the blade at Z-axis at α=15°.
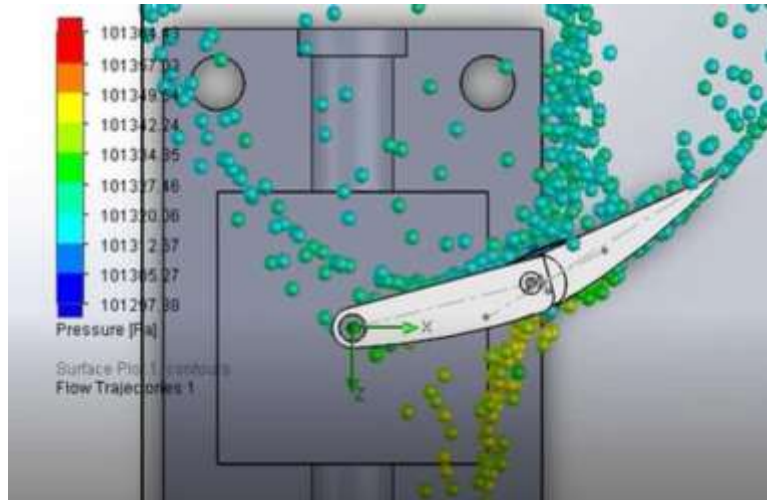
Figure 5.10 Pressure analysis when wind hits the blade at Z-axis at α=17.5°.
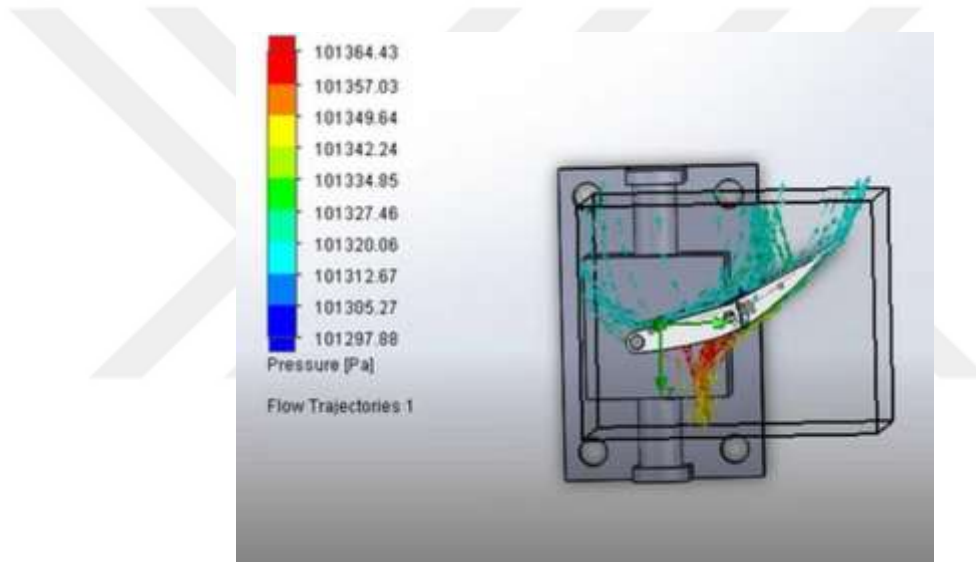
Figure 5.11 Pressure analysis when wind hits the blade at Z-axis at α=20°.
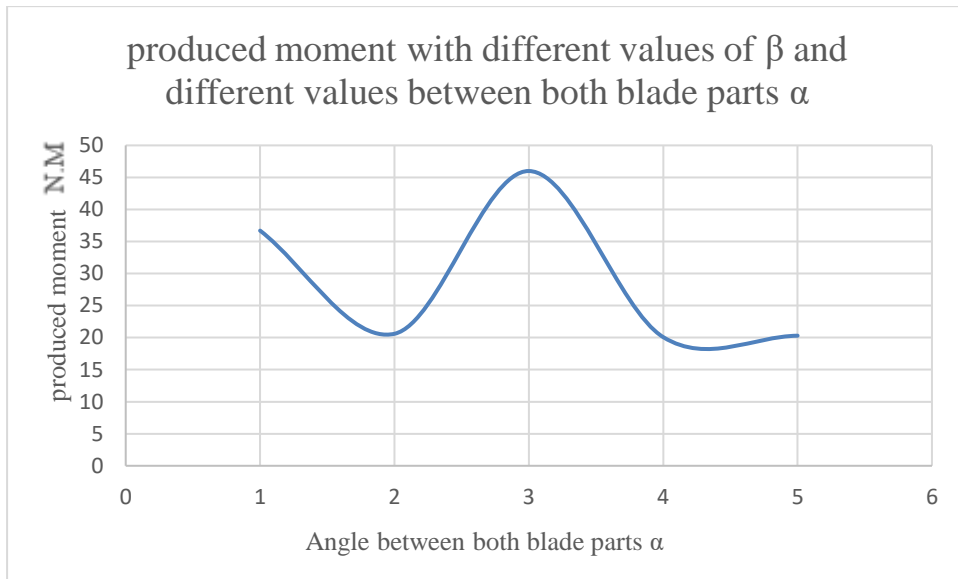
Figure 5.12 Produced moment with different values of α.

We repeat the same process fixing the angle between both parts (α = 7°) of the blade and change the angle of attack but the wind velocity of 8 m/sec. Pressures demonstrated in the fourth chapter section 4.1.2, the results support the previous inclusion where the maximum torque appears with an angle of attack equal to 24° as fig 5.14 shows.
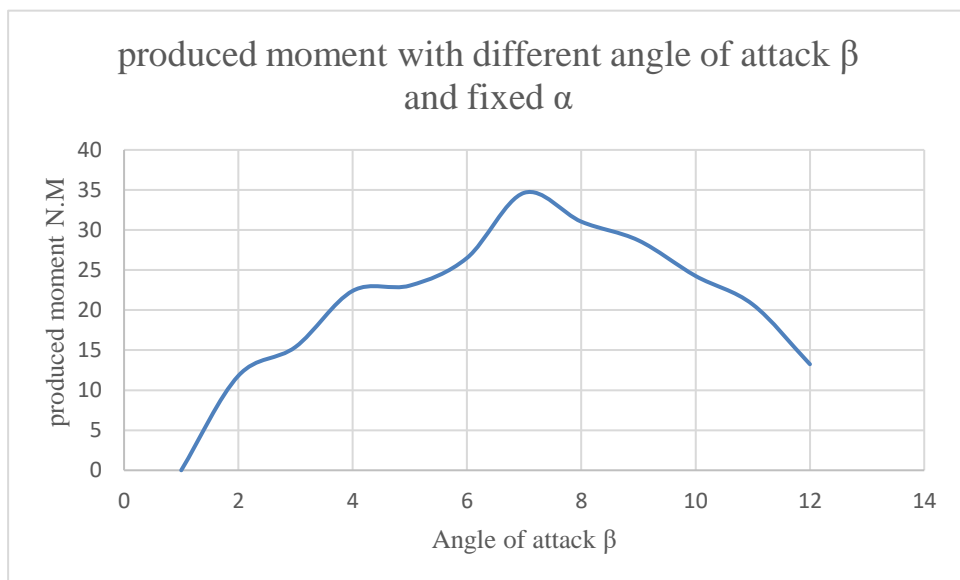
Figure 5.13 Produced moment and the angle of attack with fixed β.

The previous chart supports our idea that each wind velocity has an optimum angle of attack.

5.3 Second smart blade model

After calculation of the produced moment addressed, we will create a chart which gives the relation between surface area change and produced moment fig 5.14 explains the results.
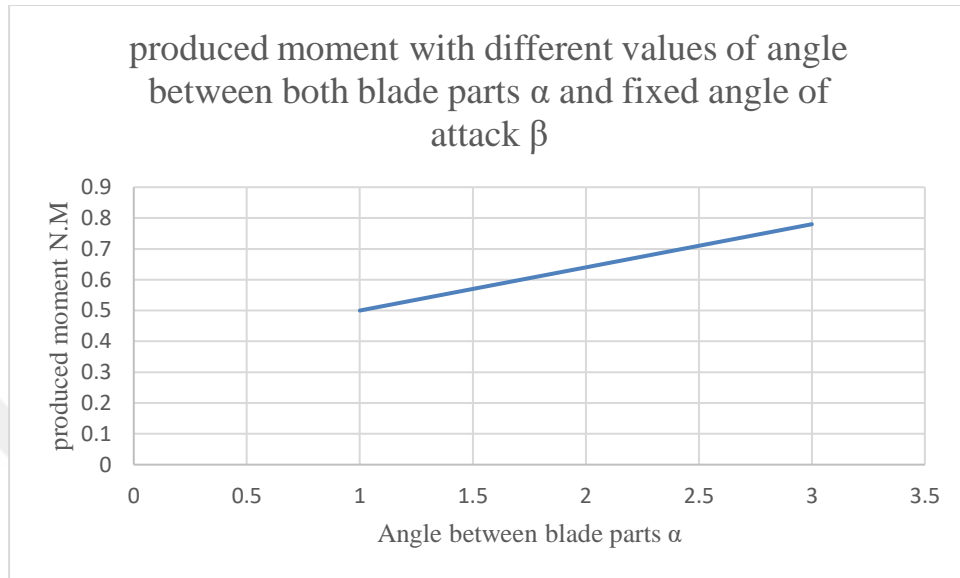
Figure 5.14 Produced moment at wind speed 8m/s with different values of α.

From the previous chart, we can recognize that when we increase the area of the wind turbine blade which facing the wind the produced moment increased. Changing the angle from 0° to 3° caused moment increase with 28% and that can be acceptable due to the incidence increasing with area. But when we moved to 6° produced moment increased up to 21%, this still theoretical results but it can be an indicator to which extent increasing the blade surface could increase wind turbine efficiency, however, this angle is the best angle because of high pressure and moment transfer.

5.4 Breaking wind turbine work limits attempts

As mentioned previously wind turbine cannot producing power when wind speed less than 5 m/sec as minimum speed and when wind speeds exceed the range of 20-23 m/sec. In some cases, a wind turbine could face blade bending or tower collapse risks, due to high wind speeds. Using our smart blades, we will try to start producing power with wind velocity equal to 3 m/s by using the second model of the smart blade and try to keep wind turbine blade able to catch wind energy when wind speeds reaches 23 m/sec without subjecting the blade to any bending risks.

5.4.1 Improve wind turbine performance at low wind speeds

At a wind speed equal to 3m/s we will repeat our experiment with three degrees between the both parts of the wind turbine blade and discover the differences in wind turbine performance when speeds became at the low limits.

First case: the angle between the both parts of the blade is equal to zero, the following results have been recorded.

Table 5.1 Forces formed on X and Y axises when α=0°.

Goal Name	Unit	Value	Averaged Value	Minimum Value	Maximum Value
GG Normal Force (X) 1	[N]	-0.21867925	-0.217676804	-0.219781824	-0.214076866
GG Normal Force (Y) 1	[N]	1.19160625	1.197377739	1.189076507	1.216831752
GG Force (X) 1	[N]	-0.21833273	-0.217397728	-0.219512226	-0.213865891
GG Force (Y) 1	[N]	1.19473135	1.200493677	1.192079422	1.220033514

$$M= 1.19*472.41*10^{-3} \rightarrow M = 0.56 \text{ N.M.}$$
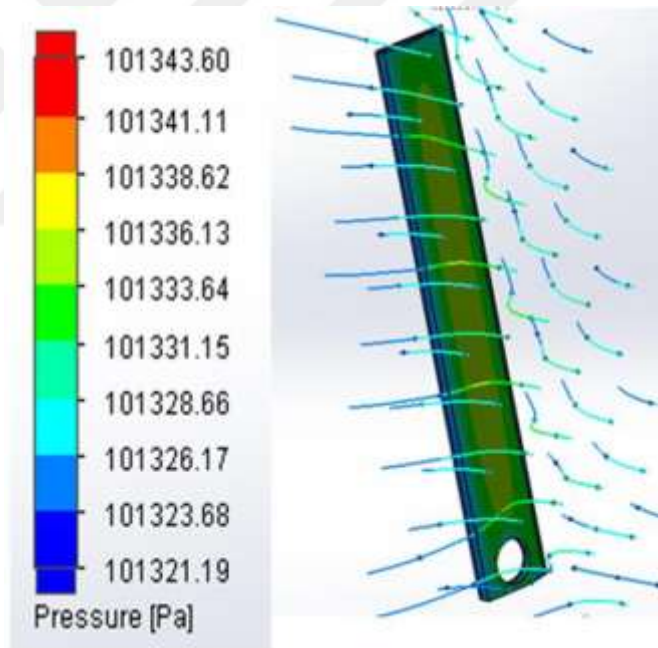
Figure 5.15 Pressure distribution and wind flow on the front face of the blade at Y-axis when α=0°.

Second case: the angle between the both parts of the blade is equal to 3°, the following results have been recorded.

Table 5.2 Forces formed on X and Y axises when α=3°.

Goal Name	Unit	Value	Averaged Value	Minimum Value	Maximum Value
GG Normal Force (X) 1	[N]	-0.23019591	-0.227840428	-0.232064726	-0.216883559
GG Normal Force (Y) 1	[N]	1.38535671	1.38631255	1.356248328	1.400647188
GG Force (X) 1	[N]	-0.22990016	-0.227467914	-0.233172019	-0.216339406
GG Force (Y) 1	[N]	1.38754779	1.388553247	1.358482539	1.40290174

$M = 1.38*472.41*10^{-3} \rightarrow M = 0.65$ N.M.
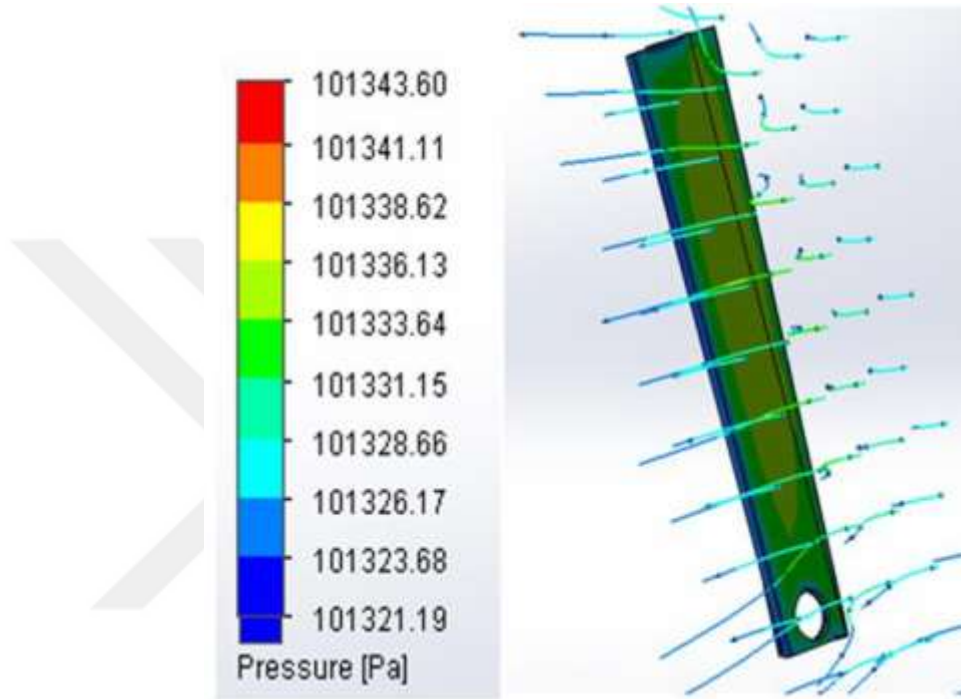
Figure 5.16 Pressure distribution and wind flow on the front face of the blade at Y-axis when α=3°.

Second case: the angle between the both parts of the blade is equal to 6°, the following results have been recorded.

Table 5.3 Forces formed on X and Y axises when α=6°.

Goal Name	Unit	Value	Averaged Value	Minimum Value	Maximum Value
GG Normal Force (X) 1	[N]	-0.26408691	-0.265366286	-0.293323258	-0.256846091
GG Normal Force (Y) 1	[N]	1.83551474	1.826674893	1.775248281	1.847812777
GG Force (X) 1	[N]	-0.26210829	-0.263337613	-0.293086065	-0.254144288
GG Force (Y) 1	[N]	1.83693421	1.828138709	1.776883794	1.849246971

$M = 1.83*472.41*10^{-3} \rightarrow M = 0.86$ N.M.

Table 5.4 Produced moment at wind speed 3m/s with different angle between blade parts.

α	Moment
0°	0.56
3°	0.65
6°	0.86
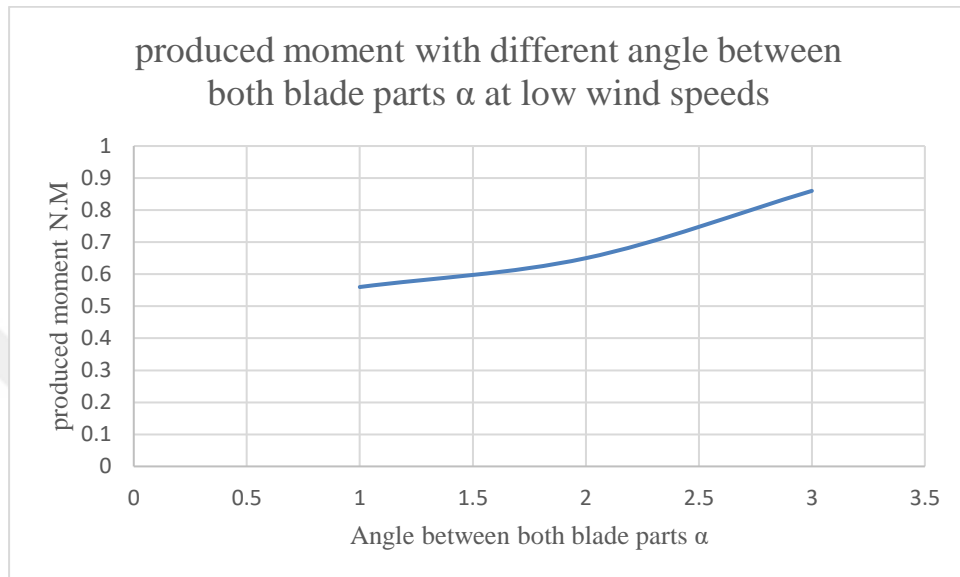
Figure 5.17 Produced moment at low wind speed 3m/s with different values of α.

If we compared between the produced moment at different wind speeds we will see that the produced moment at low wind speed 3 m/s has a very close value when wind speed was 8 m/s, which means to face decreasing wind speed velocity we will decrease the contact surface with wind which will causing continues rotation of blade at low wind speeds.

Table 5. 5 Comparing between produced moment at different wind speeds with different α.

α	Moment (N.M) Wind velocity 3 (M/S)	Wind velocity 8 (M/S)
0°	0.56	0.5
3°	0.65	0.64
6°	0.86	0.78

5.4.2 Improve wind turbine performance at high wind speeds

At a wind speed equal to 23m/s we will repeat our experiment at four different angles between both parts of the wind turbine and discover the differences in wind turbine

performance when speeds became at the high limits and agree if the wind turbine with smart blade still able to produce power using the first smart blade model.

The angle between the both parts will take the following values α = (15°, 35°, 45°, 90°).

A new method has been used in the Solid works to produce forces on the X-axis while this force will be used to calculate the moment directly using the equation (5.3).

Table 5.6 Forces formed on X and Z axises when α=15° & β= 15°.

Goal Name	Unit	Value	Averaged Value	Minimum Value	Maximum Value
GG Normal Force (X) 1	[N]	4.18692606	4.400677612	4.0465846	5.615507091
GG Normal Force (Z) 1	[N]	13.9102424	14.39792632	13.53090622	17.52288662
GG Force (X) 1	[N]	4.16052105	4.375303172	4.020130164	5.591616631
GG Force (Z) 1	[N]	13.9368137	14.42502533	13.55732788	17.55154666

M= 4.18*320*10⁻³ → M = 1.33 N.M.

Table 5.7 Forces formed on X and Z axises when α=35° & β= 15°.

Goal Name	Unit	Value	Averaged Value	Minimum Value	Maximum Value
GG Normal Force (X) 1	[N]	1.4939257	1.605503864	1.253254698	2.710837711
GG Normal Force (Z) 1	[N]	9.9630159	10.35395828	9.795778646	12.4933275
GG Force (X) 1	[N]	1.47063864	1.580053399	1.226964685	2.684762108
GG Force (Z) 1	[N]	9.99697405	10.39170764	9.832563278	12.53693668

M= 1.49*320*10⁻³ → M = 0.47 N.M.

Table 5.8 Forces formed on X and Z axises when α=45° & β= 15°.

Goal Name	Unit	Value	Averaged Value	Minimum Value	Maximum Value
GG Normal Force (X) 1	[N]	1.269067	1.623700571	1.269067005	2.477288353
GG Normal Force (Z) 1	[N]	9.4253533	10.07494582	9.425353298	11.48391555
GG Force (X) 1	[N]	1.24678494	1.599439157	1.246784943	2.444380558
GG Force (Z) 1	[N]	9.46368607	10.11876456	9.463686073	11.54749664

M= 1.27*320*10⁻³ → M = 0.40 N.M.

Table 5.9 Forces formed on X and Z axises when α=90° & β= 15°.

Goal Name	Unit	Value	Averaged Value	Minimum Value	Maximum Value
GG Normal Force (X) 1	[N]	1.6106824	1.199787559	0.740418106	1.610682395
GG Normal Force (Z) 1	[N]	11.5916471	12.2933601	11.59164709	13.23616704
GG Force (X) 1	[N]	1.59155114	1.180275814	0.72075246	1.591551144
GG Force (Z) 1	[N]	11.6064748	12.31143564	11.60647478	13.26023139

M= $1.61*320*10^{-3} \rightarrow$ M = 0.51 N.M.

Table 5.10 Produced moment when wind velocity is 23 m/s with different values of α.

α	β	Moment
15°	15°	1.33
35°	15°	0.47
45°	15°	0.40
90°	15°	0.51
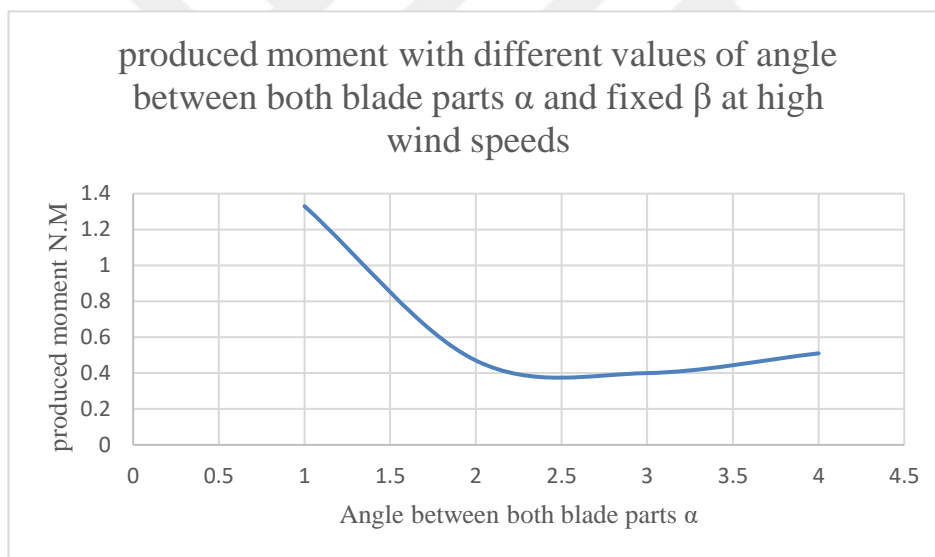
Figure 5.18 Produced moment at high wind speed 23m/s with different values of α.

From figure 5-18, we can recognize that when the angle between both parts of blade became equal to 90°, the produced moment increased if we compared it with the previous two values when the angle was equal to 35° and 45°. That gives an indicator that when we decreased contact surface with the blade of the wind turbine still able to rotate and this rotation accomplished with catching of the kinetic energy of the wind.
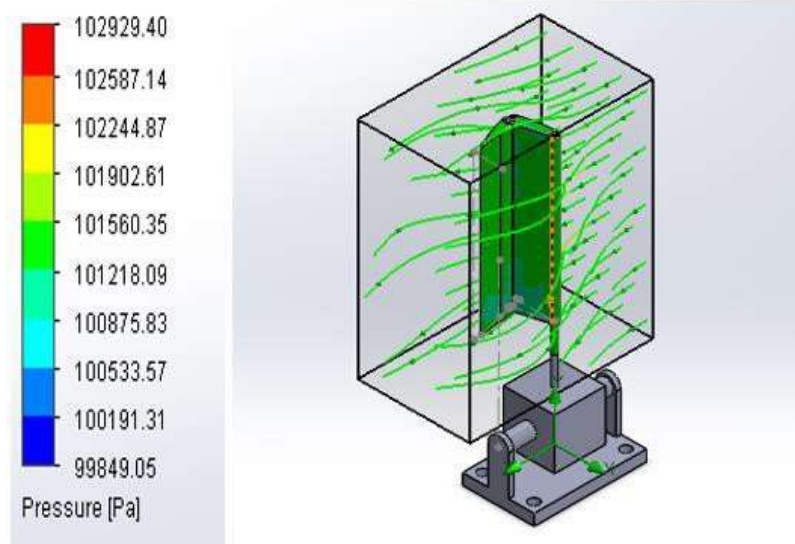
Figure 5.19 Pressure distribution and wind flow at high wind speed 23m/s and α=90°.

CHAPTER 6

CONCLUSION

Increasing wind turbine performance or increasing wind turbine efficiency can be achieved by other methods away from using a smart rotator, special control systems, blade with special flaps or increasing the size of the wind turbine which will lead to massive increase with the cost.

The previous results can be used as tangible evidence that the smart blade model is able to be used in the future of wind turbine manufacturing and able to become a real model, as well as the results agreed that this smart model affect the performance of the wind turbine positively when it accomplished with a live control system.

Utilizing the first smart blade model will be useful when wind speed is high because it will decrease the contact surface with the wind, which gives the blade the opportunity to rotate and catch kinetic energy from wind. This in contrary of the ordinary blades which are rotating without any recorded benefit at high wind speeds, in addition, decreasing the contact surface decrease the risk of bending the blade. While when wind speeds decreased to the lowest limits, the second smart blade model should be used as it offers a small contact surface with wind and still able to produce power.

Now we can move forward with the concept of the smart blades with changeable surfaces facing the wind. This research will be participating within the development of the wind turbine manufacturing and facing the variable wind conditions in different locations, in another hand, increasing power produced from wind energy will have a positive impact on the economic situation of the country and the environment.

6.1 Future work

As a future work the researcher as a first step will cover the wind turbine farms capabilities, production, and distribution in Turkey, this will support to have a better understanding of the wind turbine manufacturing in Turkey and comparing the existing wind farms outputs with the latest global attempts, this will be as a baseline study for the PhD research.

For our smart models, we will be manufacturing the first smart model as it listed in section 4.1, which tests different angle of attack. In the first phase of fixing the blade parts angle then after decided the optimum angle of attack we will start to change the angle between the both parts of the blade to reach the best angle, which will give the best performance of the wind turbine. An appropriate control mechanism should be accomplished with the smart model to enable the smart blade from taking the best angles according to wind conditions. In addition, new materials can be subjected to test to be suitable in the new models, because of materials affecting the performance of the wind turbine, both solution participating in wind turbine development attempts.

Currently, the USA is seeking to lead new technology designs and make commercial decisions while the laboratories provide theoretical and technical support through applied research and performance testing [54].

The success of this research means that the humans became able to overcome the variable condition of wind and getting benefit from kinetic wind energy as much as possible.

REFERENCES

[1]   S. Sun, S **(2016).** The, and U. States, "Types of Renewable Energy,".

[2]   K. Jager, O. Isabella, A. H. M. Smets, R. A. C. M. M. van Swaaij, and M. Zeman **(2014),** "Solar Energy Fundamentals, Technology and Systems," *Delf University Technol*ogical.

[3]   D. Elliott, M. Schwartz, R. George, S. Haymes, D. Heimiller, G. Scott, and E. McCarthy **(2001)**, "Wind Energy Resource Atlas of the Philippines".

[4]   "British Wind Energy Association Briefing Sheet **(2005)**," *Br. Wind Energy Association*.

[5]   L. C. R. U. S. D. of the I. Bureau of Reclmation **(2005)**, "Reclamation: managing water for the west," *Hydroelectr Power*.

[6]   N. Sriram and M. Shahidehpour **(2005)**, "Renewable biomass energy," *IEEE Power Engineer Soc. Gen. Meet*. 1910–1915.

[7]   N. Brandon **(2006),** "Fuel Cells," *Energy Convers"*.

[8]   K. Tromly, "Renewable Energy: An Overview," *Energy Effective. Renew. Energy Clear*.

[9]   P. A. Lincoln and New York. Times **(2012)**, "Wind generators history ©,".

[10]   G. Johnson **(2006),** "Wind energy systems," *Wind Energy System"*.

[11]   P. Tchakoua, R. Wamkeue, M. Ouhrouche, T. A. Tameghe, and G. Ekemb **(2015),** "A new approach for modeling darrieus-type vertical axis wind turbine rotors using electrical equivalent circuit analogy: Basis of theoretical formulations and model development," *Energies*.

[12]   J. Vestergaard, L. Brandstrup, and R. D. Goddard **(2004)**, "A Brief History of the Wind Turbine Industries in Denmark and the United States," *Academic. International Business (Southeast USA Chapter)*.

[13]   Hi, Qv,'ri, and @bullet **(2018)**, "DOE Large Horizontal Axis Wind Turbine Development at NASA Lewis Research Center Conservation and

Renewable Energy Wind Energy Technology Division,".

[14] J. K. Kaldellis and D. Zafirakis **(2011)**, "The wind energy (r)evolution: A short review of a long history," *Renewable Energy*.

[15] W. Energy and F. Sheet **(2001)**, "Efficiency and performance," *Wind Energy*.

[16] D. T. Mingwei Ge, Le Fang **(2015)**, "Influence of Reynolds Number on Multi-Objective Aerodynamic Design of a Wind Turbine Blade,".

[17] M. Mahmoodilari **(2012)**, "the Effect of Turbulent Flow on Wind Turbine Loading and Performance,".

[18] S. Pieralli, M. Ritter, and M. Odening **(2015)**, "Efficiency of wind power production and its determinants," *Energy*.

[19] Energy Efficiency and Renewable Energy **(2004)**, "Wind Power Today and Tomorrow,".

[20] Y. H. Qiao, J. Han, C. Y. Zhang, and J. P. Chen **(2012)**, "Modeling smart structure of wind turbine blade,".

[21] John D. Anderson, Jr **(1999)**, *Fundamentals of Aerodynamics*.

[22] A. M. Biadgo and G. Aynekulu **(2017)**, "Aerodynamic design of horizontal axis wind turbine blades,".

[23] S. Anim, Mensah **(2011)**, *The optimum design of a wind turbine blade.*

[24] K. V.j, "Towers for offshore wind turbines **(2010)**," *tenth Asian International Conference fluid machinery*.

[25] M. M. Moh Saad and N. Asmuin **(2014)**, "Comparison of Horizontal Axis Wind Turbines and Vertical Axis Wind Turbines," *IOSR J. Engineering*.

[26] M. Ragheb **(2014)**, "Components of wind machines ©," no. Mechanism of the Wind Turbine.

[27] D. Ancona and J. McVeigh **(2001)**, "Wind turbine-materials and manufacturing fact sheet," *Princet. Energy Resour. International.*

[28] M. Karimirad **(2014)**, "Offshore Energy Structures,".

[29] Renewable UK **(2000)**, "Offshore Wind Energy,".

[30] P. J. Schubel and R. J. Crossley (**2012**), "Wind turbine blade design," *Energies*.

[31] H.-J. Wagner and J. Mathur (**2013**), "Introduction to Wind Energy Systems,".

[32] A. Memon, S. R. Samo, M. Asad, and F. H. Mangi (**2015**), "Modeling of aerodynamic forces on the wind turbine blades," *J. Clean Energy Technological*.

[33] R. Balaka, A. Rachman, and J. Delly (**2014**), "Blade Number Effect for A Horizontal Axis River Current Turbine at A Low Velocity Condition Utilizing A Parametric Study with Mathematical Model of Blade Element Moment," *J. Clean Energy Technol.*1.

[34] F. Mühle, M. S. Adaramola, and L. Saetran (**2013**), "The effect of the number of blades on wind turbine wake,".

[35] M. Gaunaa, J. Heinz, and W. Skrzypiński (**2016**), "Toward an Engineering Model for the Aerodynamic Forces Acting on Wind Turbine Blades in Quasisteady Standstill and Blade Installation Situations," *J. Phys. Conf. Ser.*

[36] M. Talavera and F. Shu (**2015**), "Experimental Study of Turbulence Influence on Wind Turbine Performance,".

[37] R. E. Wilson (**1980**), "Wind-turbine aerodynamics," *J. Wind Eng. Ind.*.

[38] C.-S. Wang and M.-H. Chiang (**2016**), "A Novel Pitch Control System of a Large Wind Turbine Using Two-Degree-of-Freedom Motion Control with Feedback Linearization Control," *Energies*.

[39] Wind Energy and Power Solutions (**2015**), "Reliable Pitch Systems for Reliable Pitch Systems That Reduce the Levelized."

[40] D. Lutschinger and I. Howard (**2013**), "Experimental Tests of Wind Turbine Main Shaft Motion on a Laboratory Test Rig,".

[41] M. Zhao and J. Ji (**2016**), "Dynamic analysis of wind turbine gearbox components," *Energies*.

[42] T. C. Corke (**2018**), "Aerodynamics,".

[43] J. UKONSAARI (**2016**), *Maintenance Effect on Present and Future*

Gearboxes for Wind Turbines.

[44]   F. Oyague **(2009)**, "Gearbox Modeling and Load Simulation of a Baseline 750-kW Wind Turbine Using State-of-the-Art Simulation Codes,".

[45]   A. Ragheb and M. Ragheb **(2010)**, "Wind Turbine Gearbox Technologies," *Nuclear Renewable Energy Conf. (INREC), 2010 1st International.*

[46]   J. Peeters and J. Houben **(2012)**, "Design of wind turbine gearboxes with respect to noise,".

[47]   T. P. M. De Bazzo, J. F. Kolzer, R. Carlson, A. F. Flores Filho, and F. Wurtz **(2015)**, "Optimum design of a gearless wind turbine PMSG considering wind speed probability density function," *2015 10th International Conference Ecol. Veh. Renewable Energies.*

[48]   W. Cao, Y. Xie, and Z. T **(2012)**, "Wind Turbine Generator Technologies," *Adv. Wind Power*.

[49]   W. E. Leithead **(2016)**, "Wind Turbine Control," no. September.

[50]   M. Ragheb **(2016)**, "Control of Wind Turbines,".

[51]   J. Z. X. Xiao Chen **(2015)**, "Structural failure analysis of wind turbines impacted by super typhoon Usagiitle," *elsevier*.

[52]   E. Paramasivam, C. Robinson, E. Taylor, A. Morrison, and E. Sanderson **(2013)**, "Study and Development of a Methodology for the Estimation of the Risk and Harm to Persons from Wind turbines,".

[53]   Energy Efficiency and renewable **(2008),** U.S department of energy "20% WIND ENERGY BY 2030."